BEHAVIOR OF CHANNEL CONNECTORS IN STEEL-CONCRETE COMPOSITE BEAMS WITH PRECAST SLABS

A THESIS SUBMITTED TO
THE GRADUATE SCHOOL OF NATURAL AND APPLIED SCIENCES
OF
MIDDLE EAST TECHNICAL UNIVERSITY

BY

PINAR ARIKOĞLU

IN PARTIAL FULFILLMENT OF THE REQUIREMENTS
FOR
THE DEGREE OF MASTER OF SCIENCE
IN
CIVIL ENGINEERING

DECEMBER 2019

Approval of the thesis:

BEHAVIOR OF CHANNEL CONNECTORS IN STEEL-CONCRETE COMPOSITE BEAMS WITH PRECAST SLABS

submitted by **PINAR ARIKOĞLU** in partial fulfillment of the requirements for the degree of **Master of Science in Civil Engineering Department, Middle East Technical University** by,

Prof. Dr. Halil Kalıpçılar
Dean, Graduate School of **Natural and Applied Sciences** _____

Prof. Dr. Ahmet Türer
Head of Department, **Civil Engineering** _____

Prof. Dr. Cem Topkaya
Supervisor, **Civil Engineering, METU** _____

Examining Committee Members:

Prof. Dr. Kağan Tuncay
Civil Engineering Dept., METU _____

Prof. Dr. Cem Topkaya
Civil Engineering, METU _____

Prof. Dr. Özgür Kurç
Civil Engineering Dept., METU _____

Prof. Dr. Eray Baran
Civil Engineering Dept., METU _____

Assoc. Prof. Dr. Saeid Kazemzadeh Azad
Civil Engineering Dept., Atılım University _____

Date: 25.12.2019

I hereby declare that all information in this document has been obtained and presented in accordance with academic rules and ethical conduct. I also declare that, as required by these rules and conduct, I have fully cited and referenced all material and results that are not original to this work.

Name, Surname: Pınar Arıkoğlu

Signature:

ABSTRACT

BEHAVIOR OF CHANNEL CONNECTORS IN STEEL-CONCRETE COMPOSITE BEAMS WITH PRECAST SLABS

Arıkoğlu, Pınar
Master of Science, Civil Engineering
Supervisor: Prof. Dr. Cem Topkaya

December 2019, 87 pages

The use of precast decks in steel-concrete composite construction offers variety of advantages. Research to date has mostly focused on the use of headed stud anchors with hollow core precast decks for building structures. A large number of connectors has to be used when headed studs are employed, which increases the labor required to fill the spaces with grout or mortar. In this thesis a new system is proposed where the headed stud anchors are replaced with channel connectors. The use of channel connectors enables the reduction of the number of connectors. The proposed system has been studied through a two-phase experimental program. In the first phase, 20 push-out tests were conducted on channel connectors embedded in grout or mortar with different strengths. The size of the channel section and its width were considered as the prime variables. The test results showed that the channel connectors embedded in grout or mortar behave similar to conventional systems where the channel connectors interact with in-situ concrete. In the second phase, 4 full scale composite beam tests were conducted for proof-of-concept where the degree of composite action was the prime variable. The test results showed that the proposed system offers strengths similar to conventional fully or partially composite beams and can be an alternative to the existing composite systems.

Keywords: Composite Construction, Channel Shear Connector, Precast Deck, Push-out Test, Beam Test

ÖZ

PREKAST DÖŞEMELİ ÇELİK-BETONARME KOMPOZİT YAPILARDA U-PROFİL BAĞLANTI ELEMANLARININ DAVRANIŞI

Arıkoğlu, Pınar
Yüksek Lisans, İnşaat Mühendisliği
Tez Danışmanı: Prof. Dr. Cem Topkaya

Aralık 2019, 87 sayfa

Prefabrik döşemelerin çelik-beton kompozit konstrüksiyonunda kullanılması çeşitli avantajlar sunar. Bugüne kadar yapılan araştırmalar, çoğunlukla bina yapıları için standart başlı saplama dübellerinin boşluklu prekast döşeme ile kullanımına odaklanmıştır. Standart başlı saplamalar kullanıldığında çok sayıda bağlantı kullanılmalıdır, bu da boşlukları harç veya harçla doldurmak için gereken emeği arttırır. Bu tez çalışmasında, başlı saplama bağlantılarının u-tipi kesme bağlantılarıyla değiştirildiği yeni bir sistem önerilmiştir. U-tipi kesme bağlantılarının kullanımı, bağlantı sayısını azaltmayı sağlar. Önerilen sistem iki fazlı deneysel bir program aracılığıyla çalışılmıştır. İlk aşamada, çeşitli dayanımlardaki harç veya rötresiz tamir harcı içine gömülmüş u-tipi kesme bağlantıları ile 20 itme testi yapılmıştır. U-tipi kesme bağlantısının boyutu ve genişliği, ana değişkenler olarak kabul edilmiştir. Test sonuçları, harç veya rötresiz tamir harcı içine gömülmüş u-tipi kesme bağlantılarının, u-tipi kesme bağlantılarının yerinde dökme beton ile etkileşime girdiği geleneksel sistemlere benzer davrandığını göstermiştir. İkinci aşamada, kompozitlik derecesinin birincil değişken olduğu kavram ispatı için 4 tam ölçekli kompozit kiriş testi yapılmıştır. Test sonuçları, önerilen sistemin tamamen veya kısmen kompozitlik derecesine sahip geleneksel kirişlere benzer kapasiteler sunduğunu ve mevcut kompozit sistemlere alternatif olabileceğini göstermiştir.

Anahtar Kelimeler: Kompozit Yapı, U Tipi Kesme Bağlantısı, Prekast Döşeme, İtme Testi, Kiriş Testi

To my grandmother and grandfather in heaven

Rahmiye Korkmaz and Fahrettin Korkmaz

ACKNOWLEDGEMENTS

In the first place, I would like to offer my gratitude to my thesis supervisor Prof. Dr. Cem Topkaya due to his immense knowledge, patience, and invaluable guidance throughout this study. There is no way to express my gratitude to Prof. Dr. Cem Topkaya since this thesis could not have been possible without him.

Special thanks go to Prof. Dr. Eray Baran for his valuable guidance and foresight. He supported me in every aspect throughout my entire graduate study, so I appreciate his help.

I would also like to thank the other thesis examining committee members, Prof. Dr. Kağan Tuncay, Prof. Dr. Özgür Kurç and Assoc. Prof. Dr. Saeid Kazemzadeh Azad for their insights and valuable suggestions.

I thank Özgür Paşaoğlu, Emre Haspolat, Sinan Fırat Dal, Orhan Veli Kadı and Emre Kavak for their support. I am grateful to have these five people standing by my side.

Finally, I wish to express my most profound appreciation to two very special people, Tülay Arıkoğlu and Şerife Korkmaz. There is only one person in the world who did not get a wink of sleep for countless nights for my work motivation, my dear mother Tülay Arıkoğlu. There are none, but one more person who supported me both financially and spiritually in every sequence of my life, my noble aunt Şerife Korkmaz. They showed me how to become a strong woman in spite of all difficulties in this world. I thank both of them for being a part of my life.

This study was supported through the fund (BAP-YLT-303-2018-3691) from the Faculty of Natural and Applied Sciences of Middle East Technical University. This support is gratefully acknowledged.

TABLE OF CONTENTS

LIST OF TABLES

TABLES

LIST OF FIGURES

FIGURES

CHAPTER 1

INTRODUCTION

1.1. Steel-Concrete Composite Beam Behavior

Composite members can be formed by using steel and concrete together. The main reason for this material selection is that steel and concrete complement each other by utilizing compressive strength of concrete and tensile strength of steel.

Composite beams under flexure are efficient members. Under flexural loading, the weakness of concrete in tension is compensated by steel. Similarly, the instability types of limit states for steel under compression are compensated by concrete (Viest et al., 1997). This complementary behavior of steel and concrete provides higher strength and stiffness even with small steel sections than the non-composite counterparts do. Smaller steel section offers a cost efficient structure, as well. Therefore, steel-concrete composite beams have advantages in terms of structural parameters like higher load capacity, rigidity and economical parameters like minimized material cost.

Steel and concrete are compatible with each other because they have the same thermal expansion, and concrete provides corrosion protection and thermal insulation to the steel. In addition to these, concrete can restrain slender steel sections from local or lateral-torsional buckling. Since steel and concrete compensate each other's shortcomings, engineers are increasingly designing steel-concrete composite girders instead of using either material alone. Moreover, a steel beam is able to carry dead weight of steel and concrete by itself or it can be supported with the help of temporary props until concrete has hardened in some cases. For this reason, there is no additional requirement for expensive falsework and formwork during steel-concrete composite construction.

A representative composite girder figure with steel beam and concrete slab is indicated in Figure 1.1. The deck of a composite girder can be a plain concrete, reinforced concrete, metal deck, or anything else, but plain concrete leads to premature concrete-related splitting failures.

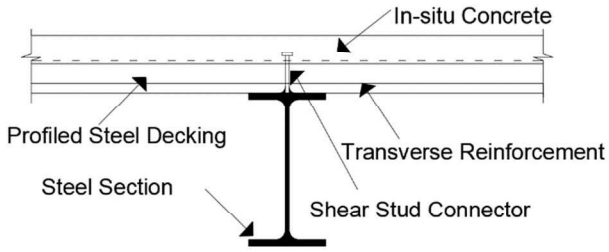

Figure 1.1. A representative composite girder

Plastic design method and partial interaction theory are used for composite beam design. For this reason, the design of composite buildings and bridges is a complicated issue. However, this minor drawback can be outweighed by the advantages of steel-concrete composite beams mentioned above due to their high resistance and ductility.

The use of steel-concrete composite construction started in the twentieth century. The interaction between these two main materials from the natural bonding was a concern in the earlier stages. Composite beam tests in US, Europe, and UK between 1923 and 1939 without any shear connection resulted with an efficiently interaction. However, these composite beams failed as soon as slip occurred at the interface of steel and concrete. Therefore, it is decided that the weak frictional bond should be remedied by mechanical connectors. The need for mechanical shear connectors used between steel and concrete in composite structures emerged in this way.

1.2. Shear Connection

When steel and concrete are used together without any connectors, slip occurs freely between these two components, and each one acts independently. As the slip at the interface between steel beam and concrete deck is minimized, the members act as a

whole. As the slip decreases, the degree of composite action increases as seen in Figure 1.2. The degree of interaction is based on the degree of shear connection.

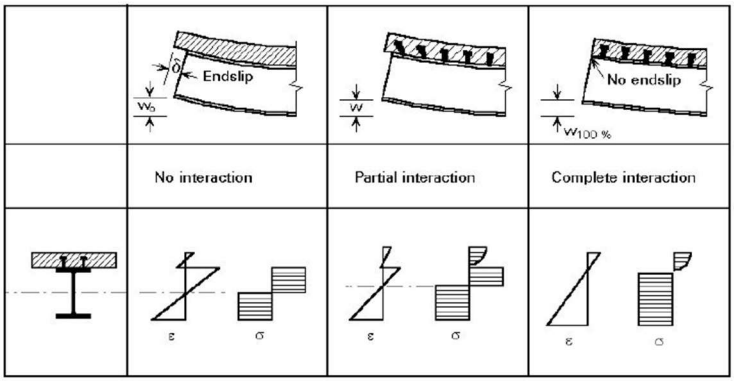

Figure 1.2. Degree of composite action (SSEDTA(European Steel Computer, 2005)

Partial composite action is usually preferred instead of complete composite action due to its lower cost. The stresses developed on a typical cross section are given in Figure 1.3 for both the cases.

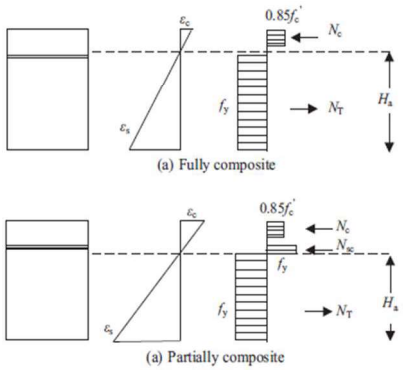

Figure 1.3. Fully and partially composite beams (Liu, Guo, Qu, & Zhang, 2017)

Composite action is formed by placing mechanical connectors between steel and concrete. This connection is called as shear connection since the main aim of this link is to restrain longitudinal shear and uplift of concrete deck. When composite action between steel and concrete is achieved partially or completely, the shear load transfer at the interface is obtained by adhesion, friction and bearing mechanisms according to Viest et al. (1997). As adhesion and friction are neglected during design, bearing is taken as the only one criterion of a reliable connection principle between two main

counterparts. Therefore, there are two main requirements shear connectors have to fulfill. First one is that shear connectors should transfer longitudinal shear forces from steel to their base; i.e. they should resist the horizontal shear forces occurring at the steel-concrete interface. Second one is that these connectors should form a tension link to the concrete, i.e. they should prevent the separation of steel and concrete. Ultimately, every shear connector should have some parts which resist direct shear force and some others which resist tension loads between steel and concrete.

Shear connectors act as dowels in concrete, i.e. they provide resistance in both vertical and horizontal directions when they are embedded in concrete. Thanks to this dowel action, shear connectors provide both direct shear transfer between steel and concrete and resist to vertical separation of concrete from steel at the same time as stated by Qureshi et al. (2011). This load principle is given in Figure 1.4. The strength and ductility of shear connectors are determined experimentally because of their complicated dowel action. For this reason, composite beam tests are done to see the behavior of shear connectors since the force capacity on shear connector is not only directly proportional to the load applied on the long composite beam, but also depends on the stiffness of other components of composite beam as stated by Lam et al. (2000). Moreover, beam tests are conducted to see the entire behavior of the structure with variable degrees of composite action. After shear force at the interface of the steel beam and concrete overcomes friction and bonding forces, the behavior of shear connection converts full interaction into partial interaction.

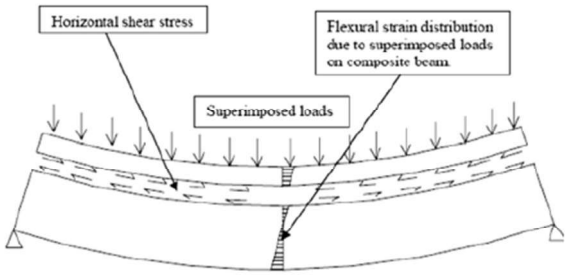

Figure 1.4. Development of shear forces during composite action (Al-darzi & Chen, 2006)

In a typical pushout test setup, shear connectors are welded to the flanges of an I-shape steel member. Then, concrete is placed next to both flanges of the steel section to create the main slab on the steel, so the shear connector is embedded in concrete and creates dowel action. The slip between concrete and steel is examined during loading until failure. The shear connector or the surrounding concrete can fail in a typical push-out test. Mostly, the load-slip relationship is taken at the end of the test, so the strength and ductility of connector can be interpreted. According to Eurocode 4 the characteristic slip value should be at least 6 mm at the time of characteristic load level, which is taken as 90% of failure load.

There are various types of shear connectors, but standard welded headed shear studs are the most common ones without a doubt. The reason of the popularity of headed shear studs is based on their proven performance and ease of application. However, this type of shear connector requires special welding equipment, and a large number of them is required to reach to the desired bending strength.

1.3. Channel Shear Connectors

There are many types of shear connectors, and some of them can be seen in Figure 1.5. These connectors can be embedded in the concrete or they can be used with precast deck by grouting around the connectors. One of the alternatives is channel shear connector, which has higher load capacity than headed studs, and can be welded on steel beams using conventional equipment unlike headed studs. Hence channel shear connectors deserve popularity in recent research about connection in steel-concrete composite beams.

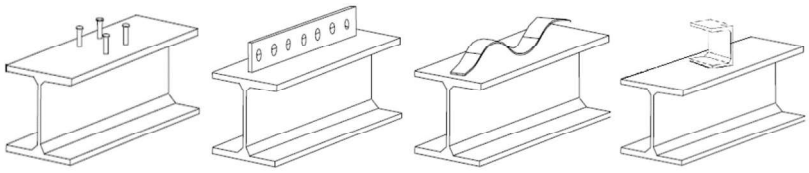

Figure 1.5. Headed studs, Perfobond ribs, Waveform strip, and channel shear connector, respectively. (Ali Shariati, 2012)

Channel shear connectors have some advantages compared to standard headed studs, and these advantages are effective not only on structural parameters, but also cost and time limitations. To begin with, channels have higher force capacity thereby providing the same strength with less number of connectors than headed studs as stated by Baran et al. (2012). It provides that the construction or rehabilitation can be completed with less cost due to the decrease of labor work and consumables, and less time. To reduce the site work increases the controlled and safer construction, as well. It should be certainly emphasized that the time and cost profits become crucial in the competitive environment of this century. Moreover, conventional welding applied for channel shear connectors is a more reliable procedure than welding with a special gun used for headed studs.

It is clear enough that channel shear connectors cover the drawbacks of standard headed studs. However, the studies on headed studs dominate the literature on shear connection in steel-concrete composite beams. That is why the studies on channel shear connectors are barely found. Some of the published research about channel shear connectors is mentioned below. The study of Viest et al. (1952) based on the classical push-out tests on channel shear connectors formed the basis of studies on this subject. The test results showed that section dimensions, i.e. flange and web thickness, and width of the channels are effective on the behavior of shear connection. However, the orientation of load whether channel loaded from its front or backside hardly makes a difference on the behavior of connection.

One of the recent valuable studies about channel shear connectors belongs to Pashan and Hosain (2009). This research gave valuable information about channel shear connectors based on the push-out tests. For instance, the test setup was prepared by cutting the I-beam to cast the concrete flanges on both flanges separately at the same time as seen in Figure 1.6, and the companion T-sections of the steel beam were welded back together. It was challenging due to much labor works, but meaningful to get the same structural properties for each concrete slab.

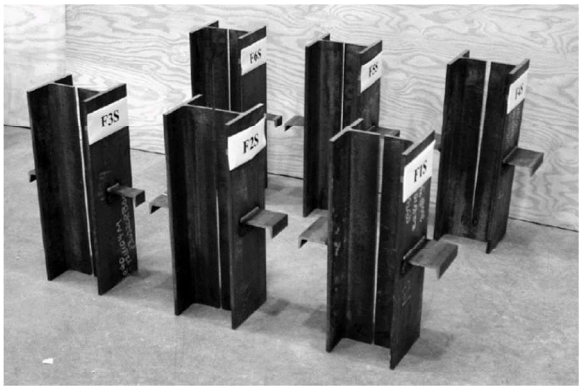

Figure 1.6. The I-beams cut to place concrete decks at the same time (Pashan & Hosain, 2009)

The concrete failure and channel failure gives different load-slip curves as seen in Figure 1.7. Channel failure leads a brittle behavior while concrete failure leads a ductile one. The increase in concrete strength results in a channel failure. In addition, the load capacity of the channel was found to be directly proportional to the channel length. Channel heights varied from 50 to 150 mm, and channel height varied from 102 mm to 127 mm. It means that the channel strength equation found at the end of this study does not cover all of the channel dimensions (Pashan & Hosain, 2009). It was found that the shear capacity is influenced by the dimensions, type and the number of connectors.

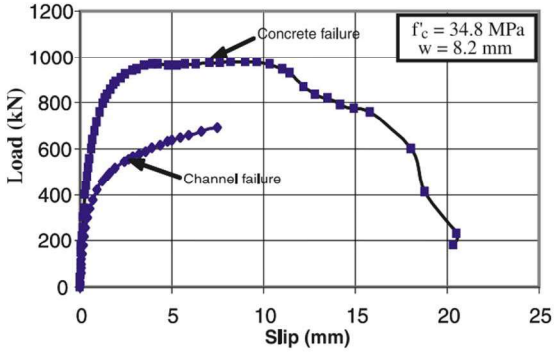

Figure 1.7. The comparison of concrete failure and channel fracture in terms of ductility (Pashan & Hosain, 2009)

The angle and channel shear connectors were compared in the study of Shariati et al. (2013). In conventional push-out tests, connector fracture occurred in both channel and angle connectors. However, the ductility and load capacity of channel shear

connectors were reported to be higher than the capacity of angles, so selecting channels seems is a better alternative (Shariati et al., 2013).

1.4. Study on Channel Shear Connectors by Baran and Topkaya in 2012-2014

This section consists of the experimental studies of Baran and Topkaya from 2012 to 2014. The advantages of channel shear connectors such as easy welding and higher force capacity thereby providing the same strength with less number of connectors than headed studs are obvious. However, the previous studies focused on North American channel connectors, so the behavior of European counterparts is unknown. For this reason, the specimens with European channel shear connectors embedded in reinforced concrete slabs were investigated using push-out tests and composite beam tests at Atılım University, respectively by Baran and Topkaya.

1.4.1. Push-out Tests (2012)

The previous studies on channel shear connectors should be extended in terms of parameter range especially on the height of channel shear connectors and more conservative resistance equation with wider data set. Baran and Topkaya performed push-out tests on channel type shear connectors for these purposes in 2012.

1.4.1.1. The Test Setup

In standard push-out test setup, concrete is placed on both flanges of steel I-beam at different times, so the time difference of casting between these two sides give rise to different concrete compressive strength. Therefore, the strength incompatibility is inevitable. Pashan and Hosain (2009) came up with a solution to this complication by cutting the I-beam along the web and weld them back after casting concrete on both flanges at the same time. This method worked against the drawbacks of conventional

test setup admittedly, but it was challenging due to additional labor works and cost. Therefore, Baran and Topkaya (2012) used another test setup in their study to eliminate the difficulties of other setup types. The push-out test setup used in the study of Baran and Topkaya (2012) can be seen in Figure 1.8.

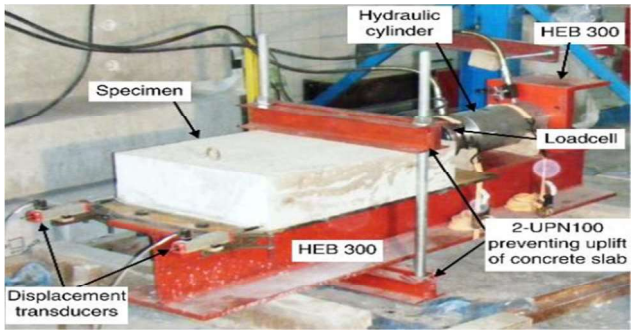

Figure 1.8. The horizontal push-out setup (Baran & Topkaya, 2012)

A similar test setup was reported in another study of Topkaya in 2004 as seen in Figure 1.9 (Topkaya, Yura, & Williamson, 2004). Therefore, it can be said that the test setup seen in Figure 1.8 is an updated version of the setup used from Topkaya in 2004. The need of this novel test setup had arisen due to the inadaptability of early-age concrete to the standard one. The early-age specimens should not be moved or anchored to prevent damage, so this original test setup was formed, and the capacities of studs embedded in concrete in composite structures at early concrete ages from 4 hours to 28 days were studied. In addition to them, the push-out setup can be changed based on the conditions as seen this study, but in fact, the single-sided push-out tests reduce the experimental cost by overcoming the inefficient duplication of two identical slabs.

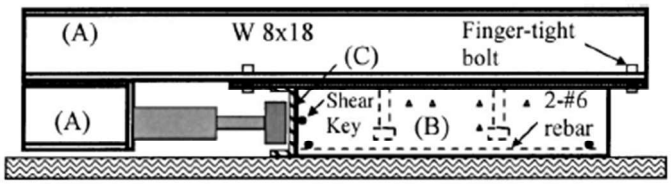

Figure 1.9. Push-out test setup (Topkaya et al., 2004)

1.4.1.2. Parameters

The tests have variable parameters which are channel height and length as a whole and these parameters can be investigated in Table 1.1. By adopting various channel sizes, it was possible to change the flange thickness and depth of the channel. Lengths of 50, 75, and 100 mm were investigated. Some of the specimens employed double channel connectors while most of the specimens employed a single one. The results of the coupon tests to determine material properties are indicated in Table 1.2. The heights of the European channels varied from 65 mm to 140 mm.

Table 1.1. The properties of specimens (Baran & Topkaya, 2012)

Specimen	Number of channel connectors	Channel size	Channel height, H (mm)	Channel length, L_c (mm)	Concrete strength, f'_c (MPa)
S65-50	1	UPN 65	65	50	31.8
S80-50		UPN 80	80	50	33.3
S100-50		UPN 100	100	50	32.2
S120-50		UPN 120	120	50	39.9
S140-50		UPN 140	140	50	36.7
S65-75		UPN 65	65	75	34.7
S80-75		UPN 80	80	75	33.8
S100-75		UPN 100	100	75	36.7
S120-75		UPN 120	120	75	32.7
S140-75		UPN 140	140	75	32.9
S65-100		UPN 65	65	100	34.0
S80-100		UPN 80	80	100	34.5
S100-100		UPN 100	100	100	33.4
D65-50	2	UPN 65	65	50	34.6
D80-50		UPN 80	80	50	33.9

Table 1.2. The geometric and material properties of channel sections (Baran & Topkaya, 2012)

Channel size	H (mm)	b_f (mm)	t_w (mm)	t_f (mm)	F_y (MPa)	F_u (MPa)	Maximum elongation (%)
UPN 65	65	42	5.5	7.5	422	501	22
UPN 80	80	45	6.0	6.0	364	467	33
UPN 100	100	50	6.0	8.5	332	470	33
UPN 120	120	55	7.0	9.0	344	465	33
UPN 140	140	60	7.0	10.0	318	451	35

H: Height t_w: Web Thickness F_y: Yield Strength
t_f: Flange Thickness F_u: Tensile Strength

1.4.1.3. Results

The test results show that the failure was due to channel fracture in all of the specimens. The typical deformation pattern of channel shear connectors was on the fillet between web and flange welded to the steel beam as seen in Figure 1.10. However, as channel length increased concrete cracking was observed.

Figure 1.10. Typical deformation pattern of channel shear connectors (Baran & Topkaya, 2012)

The load-slip relationships were obtained, so the strength and deformation capacity of channels can be interpreted with respect to channel height and length. The channel capacity increases with channel size and width as expected. However, neither channel height nor channel length influence initial stiffness significantly. The direct proportion

between channel height and push-out load capacity, and the counterpart between channel length and capacity can be seen in Figure 1.11 and Figure 1.12, respectively.

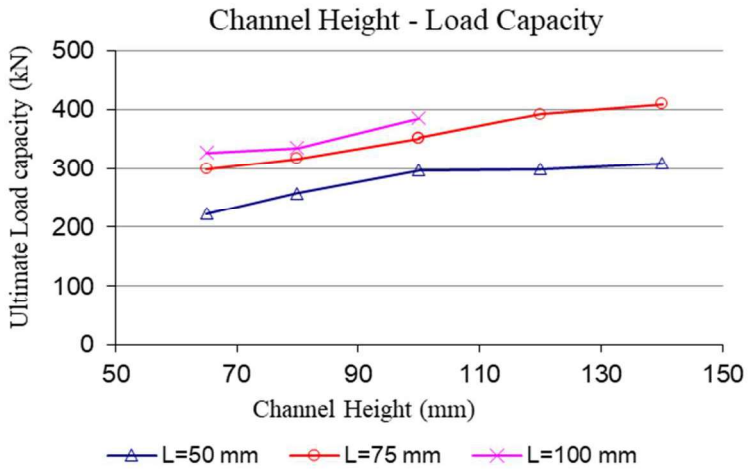

Figure 1.11. Relationship between channel height and load capacity (Baran & Topkaya, 2012)

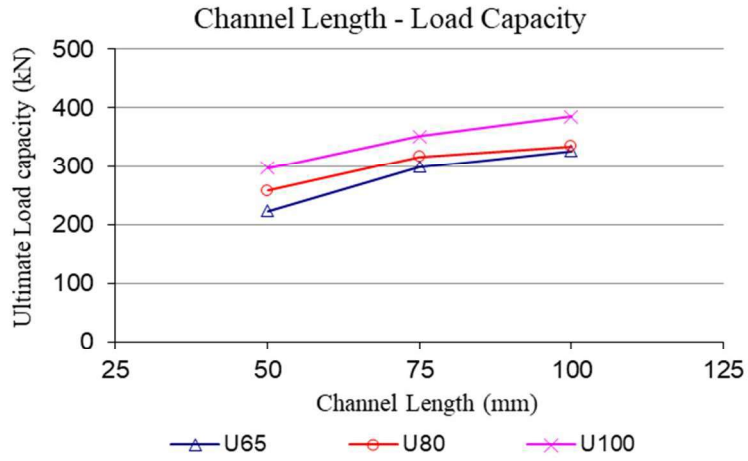

Figure 1.12. Relationship between channel length and load capacity (Baran & Topkaya, 2012)

1.4.1.4. Assessment of Code Provisions based on Push-out Tests

American and Canadian design codes recommend equations for the nominal strength of channel shear connectors. The strength formulation for prediction of channel connectors provided by American Institute of Steel Construction Specification (AISC)

and Canadian standard CAN/CSA-S16-01 are given in Eq.1.1 and Eq.1.2, respectively. Pashan and Hosain (2009) also developed an empirical equation to predict the ultimate strength of channel shear connector which is indicated in Eq.1.3. This equation takes the effect of the height of the channel shear connectors into account.

$$Q_n = 0.3 \times (t_f + 0.5t_w) \times \sqrt{f_c'} \times E_c \qquad (1.1)$$

$$Q_n = 36.5 \times (t_f + 0.5t_w) \times \sqrt{f_c'} \qquad (1.2)$$

$$Q_n = (336 \times t_w + 5.24 \times L_c \times H) \times \sqrt{f_c'} \qquad (1.3)$$

where,

Q_n = nominal strength of a channel shear connector embedded in a solid concrete slab (N)

t_f = flange thickness of channel shear connector (mm)

t_w = web thickness of channel shear connector (mm)

L_c = length of channel shear connector (mm)

f_c' = compressive strength of concrete (MPa)

E_c = modulus of elasticity of concrete (MPa).

H = height of channel shear connector (mm).

The push-out test results obtained by Baran and Topkaya (2012) were compared with these equations, and it can clearly be seen from Figure 1.13 that none of them provide consistency between predicted and measured capacity. The specified equations of American and Canadian codes result in too conservative capacity values. On the other hand, the equation proposed by Pashan and Hosain (2009) was valid only for channel heights from 102 to 127 mm, so this equation can be used for only channel section of 100 mm height when European sections are handled. Therefore, Baran and Topkaya (2012) developed a new equation given in Eq.1.4 to provide a higher accuracy.

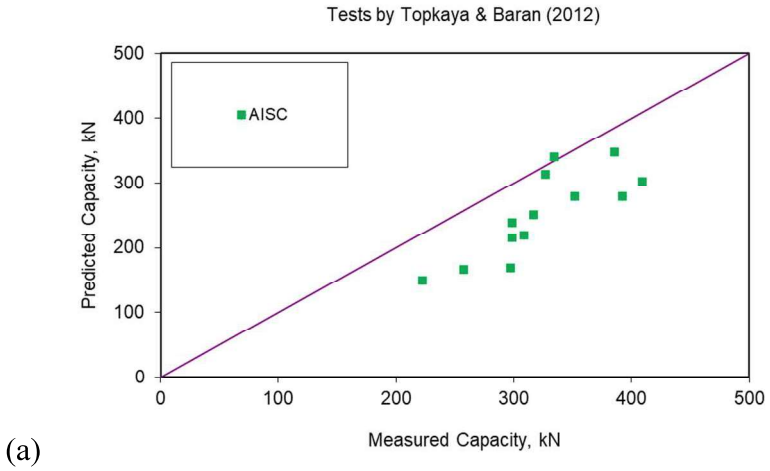

(a)

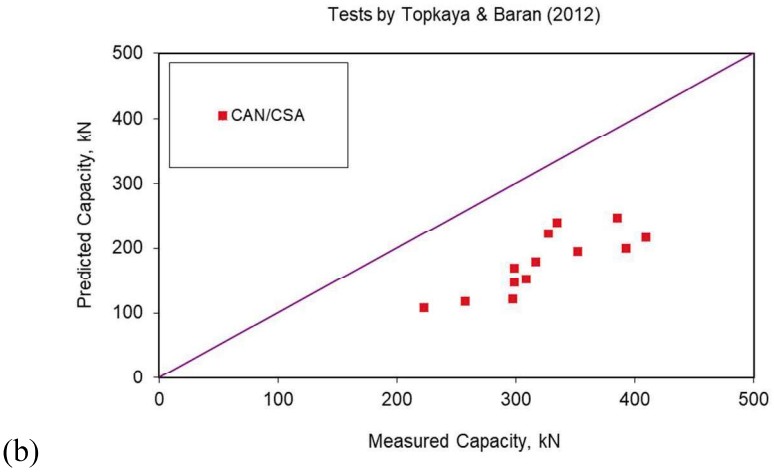

(b)

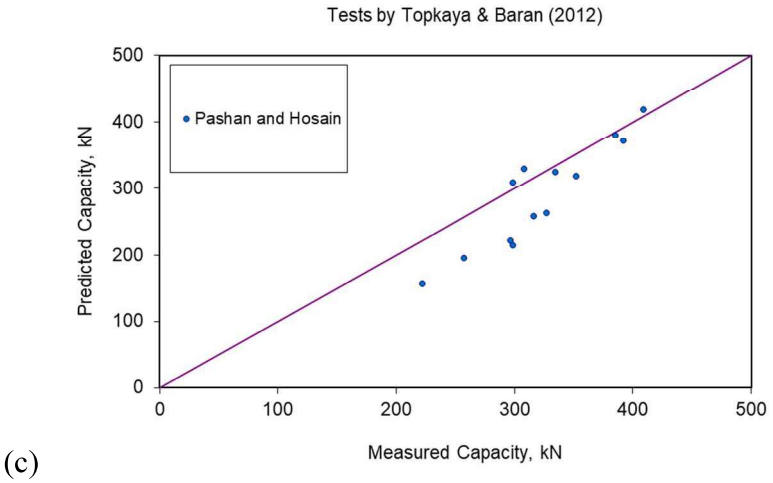

(c)

Figure 1.13. Comparison of Measured and Predicted Load Capacities: (a) American code, (b) Canadian code, (c) Pashan and Hossain (Baran & Topkaya, 2012)

$$R_n = 0.25 \times F_1 \times F_2 \times f_c' \times L_c \times H + \frac{2 \times t_w^{\,2} \times L_c}{H} \times F_u \qquad (1.4)$$

where;

$F_1 = 7.2 - 0.023.Lc$

$F_2 = 1.5 - 0.005.H$

f'_c = compressive cylinder strength of concrete (MPa)

L_c =length of channel shear connector (mm)

H = height of the channel (mm)

t_w = web thickness of channel shear connector (mm)

F_u = tensile strength of steel (MPa)

The F_1 and F_2 values in the formula represent the effect of channel length and height, respectively. The reasonable accuracy considering the push-out test results can be seen in Figure 1.14.

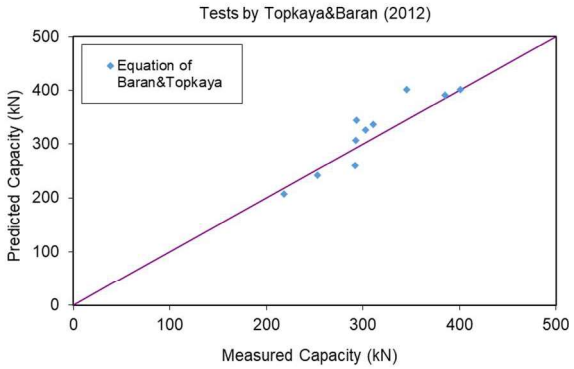

Figure 1.14. Comparison of Experimental Results and Predicted Values in accordance with Eq.1.4 developed by Baran and Topkaya (2012)

1.4.2. Beam Tests (2014)

The second phase of the study consisted of the behavior of channel shear connectors in partial composite beams. For this reason, the beam tests were conducted by using four full-scale composite beams with variable degrees of composite action. As can be seen in Table 1.3, the specimens of beam tests were a bare steel beam and four

composite beams from partial to full degree of composite action. The detailed information about the calculation of composite action can be found from the study of Baran and Topkaya (2014).

Table 1.3. Properties of specimens of beam test (Baran & Topkaya, 2014)

Specimen	Number of shear connectors per shear span	Shear connector spacing, s (cm)	Concrete compressive Strength, f'_c (MPa)	$\Sigma Q_n / F_y A_s$
B	-	-	-	-
C2	2	82.50	32.6	0.35
C3	3	55.00	33.3	0.53
C4	4	41.25	33.8	0.70
C6	6	27.50	33.3	1.06

The test setup can be seen in Figure 1.15. The number of channel shear connectors was calculated for half span along the beam, and loads were applied at single point on the beam, but the load spreader beam was also used as seen in Figure 1.16. This study had already focused on the variation of strength and stiffness with various number of shear connectors.

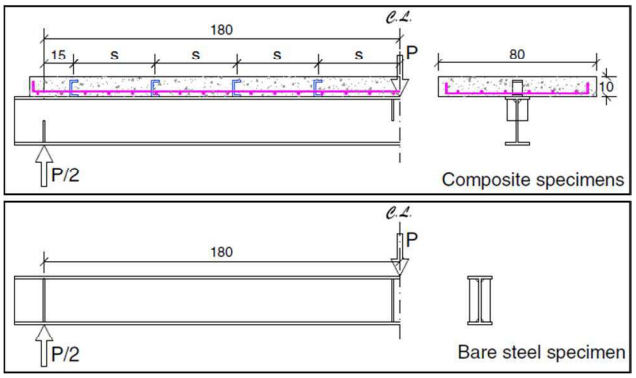

Figure 1.15. The test setup of composite beam (upper part) and bare steel beam (bottom part) (Baran & Topkaya, 2014)

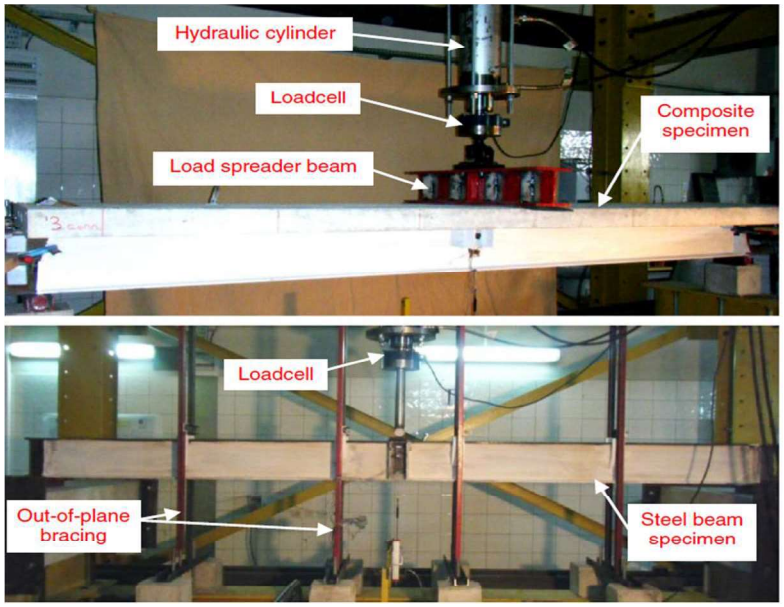

Figure 1.16. Details of test specimens of composite beam (upper part) and bare steel beam (bottom part) (Baran & Topkaya, 2014)

The results show that the moment capacity and service stiffness increase, and relative end slip decreases with increasing degree of composite action as seen in Figure 1.17, so the number of connectors is very important. It is a direct proof of superiority of the advantage of channel shear connector to have same strength to the conventional studs with less number due to its high contact area with concrete.

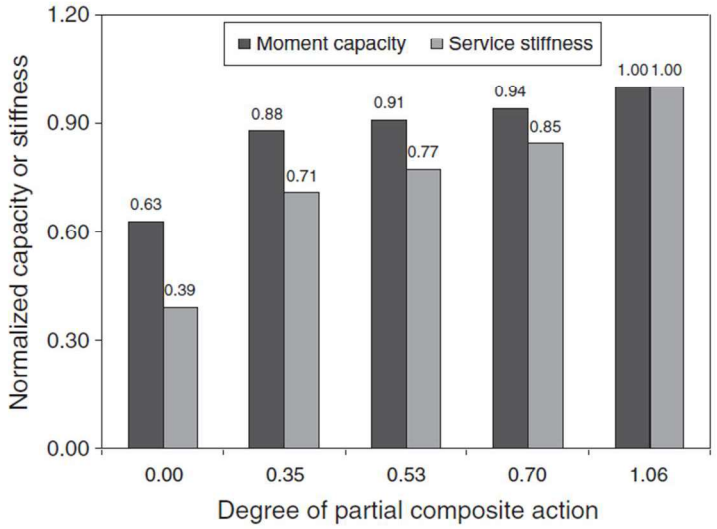

Figure 1.17. Beam response with degree of partial composite action (Baran & Topkaya, 2014)

1.5. Precast Deck Application in Composite Beams

1.5.1. Composite Beams with Precast Deck

The shear connectors mentioned above can be embedded to the concrete or they can be used with precast deck by grouting the shear pocket around connector, so the concept of precast deck is discussed in this sub-chapter in detail. Using precast deck instead of cast-in-situ ones is valuable to save cost and duration of first installation and replacement of the damaged parts, so the academic studies and innovations on precast deck system come into prominence.

A precast deck shown in Figure 1.18 has some advantages: First of all, the on-site construction operations are reduced, so wet trades are avoided. As a side note, the shear connectors are pre-welded on beams before delivery to site, thereby offering savings associated with shorter construction times. Second advantage is that traffic interference is minimized due to the reduction of in-situ concrete work. Another point worth mentioning is that high quality is ensured as the units are produced in a shop, not at the site. Small tolerances on quality of units due to the manufacturing under controlled factory conditions means a long-lasting composite beam. One more advantage of precast deck system in composite beams is about propping during construction. A few temporary formworks are already enough due to composite system. In addition to this, precast system tolerates the formwork progress a lot. Timber formwork can be altered by precast concrete elements or profiled steel sheeting. Briefly, prefabrication provides high quality and practicability.

The precast deck has some gaps to place the connectors as seen in Figure 1.18-b, so the gaps can be filled with mortar, grout or concrete to provide composite action. The hardening of the filling material is awaited, thereby giving composite action with the beams. However, careful detailing and construction practice are desired to get adequate containment for the connectors. According to this study, grout and mortar are acceptable options for easy application since they have both viscous and hardening characteristics.

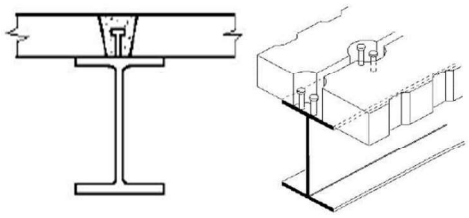

Figure 1.18. (a) Composite beam with prefabricated deck (Left), (b) A system formed by using large prefabricated deck elements with longitudinal joints (Right) (SSEDTA(European Steel Computer, 2005)

Kim et al. explained in their study (2003) that there are many types of precast concrete slab. To illustrate, full-precast concrete slabs cover the whole depth of the bridge decks whereas half-precast concrete slabs are only 70-120 mm thick and cover only the bottom half of the deck, and the top half of the deck is constructed after the bottom half (the precast concrete slabs) according to Kim et al. (2003). For this reason, full-depth precast concrete is more practical than others are, and it reduces the labor cost significantly.

Shim et al. (2001) studied on the conventional headed studs by using precast concrete deck system as seen in Figure 1.19. Non-shrinkable mortar was used as filling material in gaps of precast deck and bedding layers, and studs were placed in these gaps as shear pockets to generate shear load distribution between connectors. The results of the classical push-out tests showed that the deformation capacity of the shear connection in precast deck is higher than that in cast-in-place deck. This is very important because increasing slip capacity infers high ductility. In addition, strength of mortar is directly proportional to the ultimate capacity of connectors.

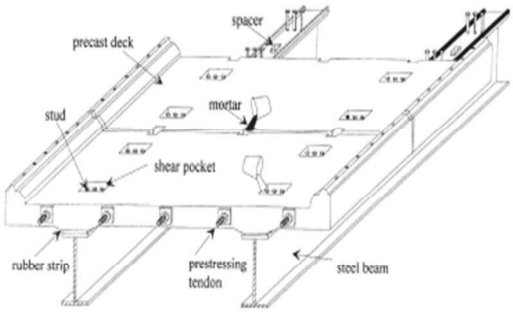

Figure 1.19. Full-depth precast deck system (C.-S. Shim et al., 2001)

The procedure of precast deck system has been summarized by Shim et al. (2001). Firstly, the deteriorated deck is removed if the process is rehabilitation, not new installation. If not, the shear connectors are welded on the top flange of the steel beam. Secondly, the girders are prepared, and precast decks are positioned. Thirdly, shear pockets are filled with grout or mortar. When the gaps around shear connectors are filled with mortar or grout, composite action begins to form. This general procedure is easy when compared with shear connection embedded in concrete at all.

1.5.2. Composite Beams with Hollow Core Slabs

Even though the hollow core slab deck in steel-concrete composite bridges is still not widespread, such types of slabs in composite beam of multistory buildings are currently being used. These precast hollow core slabs can be manufactured with continuous circular or elongated openings along their length to alter slabs internally.

Composite beams with hollow core slabs have almost all advantages of precast decks, which are mentioned above, especially reducing the erection time due to using precast units connected together at site. According to the review of Al Darzi et al. (2006), the preference of hollow core reinforced concrete slab produces some additional considerable advantages. Firstly, it decreases the self-weight of concrete, so using hollow core floor unit (HCU) provides excellent structural capacity to self-weight ratio. Secondly, it also reduces the quantities of reinforced concrete, so establishes constructions that are more economical. Thirdly, it reduces the effects of creep and shrinkage of the concrete slab, which are not negligible issues (Al-darzi & Chen, 2006).

However, connecting such precast units with the steel beam is a complex mission since it involves many details, notably availability of extra reinforcement, cast in placement slab, grouting materials, and selection of connection type. Therefore, experimental studies are needed to investigate the behavior. The studies done by Lam and others in the Civil Engineering Laboratories at Nottingham University serve for this useful

purpose. The features of test setup and results of these studies are briefly summarized below.

In the study at Nottingham University, the 150 mm deep units were attached to the universal beams through conventional welded headed studs which have 19 mm diameter, and a 6m-span was tested as composite beam under four-point bending. To begin with, the steel beam was designed in isolation from hollow core precast concrete deck, and composite action is not formed with these precast units as seen in Figure 1.20. Then, composite action was generated between hollow core precast slab and steel beam as seen in Figure 1.20. It was achieved with mechanical shear connection and in-situ filling materials. The design was optimized such that concrete deck works under compression while steel beam works under tension, so the fundamental working principle is not different from other composite beams (D. Lam, Elliott, & Nethercot, 2000b).

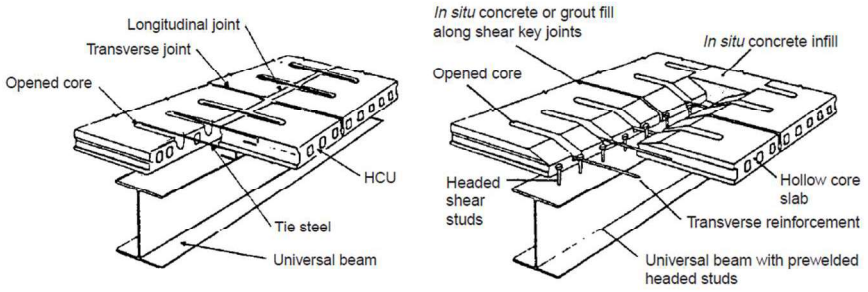

Figure 1.20. Noncomposite beam with hollow core floor unit (HCU) (Left), Composite beam with precast hollow core floor unit (HCU) (Right) (D. Lam et al., 2000b)

Hollow core slabs have longitudinal voids as seen in Figure 1.20. These longitudinal joints between units were filled with in-situ concrete or grout in order that horizontal compressive membrane forces could be transferred by the slab. Shear connectors were pre-welded to the top flange of beams, and concrete was placed around these spaces to complete composite action. The end profile of precast hollow core slabs can be seen in Figure 1.21. This application indicates that partial or full interaction between hollow core precast deck and steel beam can be achieved by adjusting material properties and suitable geometry (Dennis Lam, 2002).

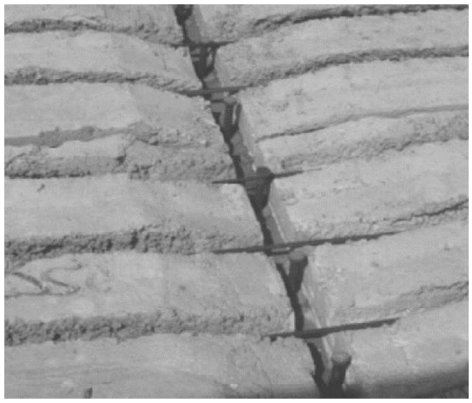

Figure 1.21. End profile of hollow core slabs (Dennis Lam, 2002)

The deck units were positioned on the top flange of the steel beam with a gap (g) as seen in Figure 1.22 of 65 mm nominal width. This width size allowed the correct compaction of concrete around pre-welded headed studs. The near end of slabs was tapered as seen again in the same figure. After positioning the transverse tie steel, the gap was filled with at least C25 in situ concrete. The main parameters of these beam tests were transverse tie steel area which range from 0.11% to 0.45% of the area of concrete, and precast in-situ concrete type.

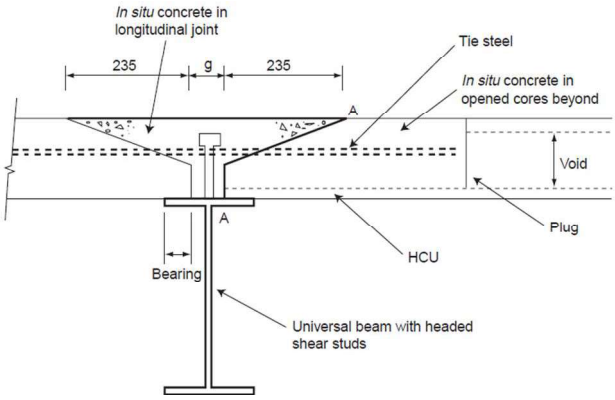

Figure 1.22. Details of precast in-situ joint of composite beam with hollow core slab units (D. Lam et al., 2000b)

The full-scale composite beam tests have shown that the composite action between hollow core slabs and steel beam was accomplished with the help of pre-welded headed studs and in-situ concrete of minimum 25 MPa of compressive strength. Moreover, test results have shown that the flexural strength of the composite beam is

between 50 and 100% higher than that of the bare steel beam. Furthermore, the flexural stiffness is 300% greater than that of the bare steel beam. These results make the profits of using hollow core precast slabs in composite beams clear enough. In addition, the reinforcement with at least 11% area of the concrete and the filling concrete of at least C25 should be used in accordance with this study, but the over reinforcement should be avoided due to brittle failure risk (D. Lam et al., 2000b).

The horizontal push-out test setup was also prepared with hollow core precast slabs. Lam et al. (2002) carried out over 100 push-out tests, and the test results indicated that the welded headed studs are affected by not only tension, but also the strength and gap width of in-situ concrete filled, the amount of transverse reinforcement, and the presence of longitudinal and transverse joint (Dennis Lam, 2002). The longitudinal shear transfer mechanism can be seen in Figure 1.23.

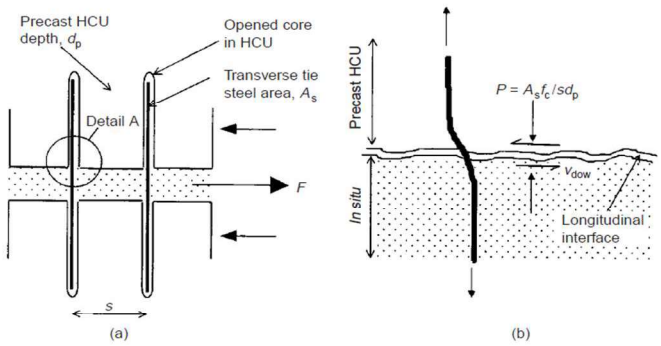

Figure 1.23. Mechanism of shear transfer, plan view (a), detail (b) (D. Lam, Elliott, & Nethercot, 2000a)

According to Lam et al. (1999), hollow core precast slabs are now the most widely used type of precast deck in Europe because of the considerable structural efficiency mentioned above. The hollow core precast decks have voids longitudinally and these voids are produced on a long pre-stressing bed. This feature makes hollow core slabs different from other precast systems in general. Additionally, a ductile failure can be obtained with correct quantities of tie steel and in-situ concrete positioned between the precast decks and around the shear studs (Lam et al., 1999).

1.6. Problem Statement and Proposed System

The literature review showed that the use of channel connectors in precast slabs has not been investigated in the past. The composite system shown in Figure 1.24 is proposed as a part of this thesis. The idea here is to develop a composite floor system where precast decks can be connected to steel beams with channel connectors. The use of channel connectors enables to use a few number of connectors to achieve composite action. Furthermore, the number of connectors can be minimized by utilizing partial composite action. Therefore, the application of this proposed system to partially composite beams requires additional research. The present study has been conducted in two phases where the first phase concentrated on push-out tests and the second phase concentrated on the composite beam tests.

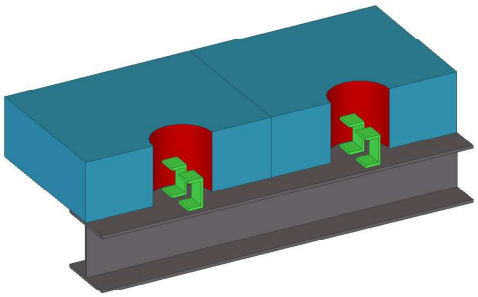

Figure 1.24. The proposed composite system

1.7. Organization of the Thesis

This thesis is organized as follows:

Chapter 1 presents the general behavior of steel-concrete composite beams, and connection to form these systems. Moreover, the past studies are mentioned, especially about composite beams generated by using precast decks and composite beams formed by using channel shear connectors. The gaps in literature and the aim of this study of thesis are also clarified.

Chapter 2 explains the first phase at the experimental program which is on the push-out tests in detail. There are several parameters designated during push-out tests, so the effect of each one are examined in accordance with the test results.

Chapter 3 explains the second phase of the experimental program which is on full-scale beam tests in detail. These tests clearly show that the connection system tried on push-out tests works in a composite beam system properly.

Chapter 4 presents a brief summary, conclusions, and some recommendations about the expectations of future researches on this subject because both shear connection and precast deck design are the essential subjects to research and progress in steel-concrete composite beams.

CHAPTER 2

PUSHOUT TESTS

This chapter describes the first phase of the experimental study which consisted of push-out tests. These tests were conducted at Structural Mechanics Laboratory of Department of Civil Engineering to examine the behavior of channel connectors embedded in mortar or grout filled pockets.

2.1. Test Specimen Design

In conventional push out tests, shear connectors are embedded in concrete blocks where the blocks are placed on two sides of a steel I-section. A similar test with a different test setup was employed in this study. Concrete blocks with a cylindrical pocket were prepared to simulate a precast deck. The channel connectors were placed inside the cylindrical pocket and the pocket was filled with mortar or grout.

The concrete for the blocks of all the specimens was placed at the same time to have consistency among specimens in terms of concrete strength. For this purpose, wooden formworks from OSB (oriented strand board) sheets were prepared such that the concrete blocks have 180 mm height and 500×700 mm base dimensions. Corrugated pipes were utilized to form the cylindrical shear pocket. This type of plastic pipe has considerable ring stiffness because it has parallel ridges and furrows that fully encircle itself. The pipes have sufficient flexibility and strength which are two necessary features to form a shear pocket. It is worth mentioning that in older studies, inclined materials were used to prevent uplift of concrete. In contrast, for this study, corrugated pipe was used because the serrated surface of this pipe also prevents uplift of concrete, so there is no need to do slant shear test which helps to decide if the bonding between the filling material and concrete is adequate or not.

The outer and inner diameters of these corrugate pipes were 175 mm and 165 mm, respectively. They were cut with a height of 220 mm, and placed in the middle of each formwork and some silicone was applied around its lower surface to make it immobilized and also to prevent the leakage. In addition, these pipes were cut along four lines and taped again as seen in Figure 2.1 to make it easy for the separation from hardened concrete. Pilot tests revealed that cutting at four sides is sufficient for easy removal.

The inner surfaces of the OSB formwork were greased to avoid hardship during removal of concrete specimens. Steel reinforcing bars were placed inside the formwork as shown in Figure 2.1. It should be noted that the reinforcement did not pass through the cylindrical pocket. The dimensions of the reinforcement are indicated in Figure 2.2. A concrete cover of 25 mm was used in all specimens.

Figure 2.1. The molds with corrugated pipes and reinforcement bars

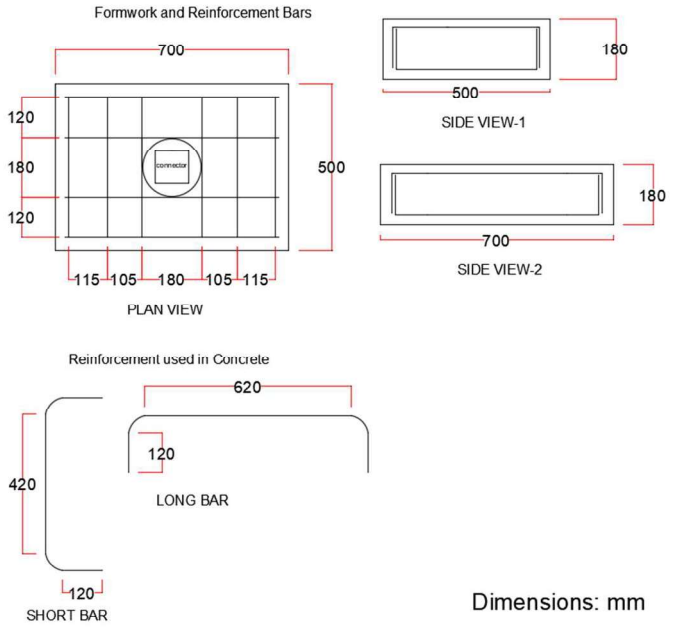

Figure 2.2. Dimensions of concrete slab and reinforcement details

The concrete of slabs was placed as ready-mix for all twenty specimens as seen in Figure 2.3. The cylinder samples with a diameter of 100 mm and length of 200 mm were also taken to determine the strength of the mixture. The cylindrical compressive capacity of concrete slab was 29.70 and 29.81 MPa at 28th day after casting and 84th day after casting which is the test day, respectively.

Figure 2.3. Concrete casting stage

After setting time of concrete has been completed, the concrete specimens were removed from OSB formwork. The corrugated pipes were separated from hardened concrete with the help of a welding torch as seen in Figure 2.4. After this operation the concrete blocks were ready to be placed over steel plates with welded channel connectors as shown in Figure 2.5.

Figure 2.4. Removal process of corrugated pipes from concrete specimen

Figure 2.5. Concrete specimens with empty shear pockets

Steel plates with 15 mm thickness, 300 mm width and 1000 mm length were used to simulate the flange of a section where the channel connectors are to be attached. Bolt holes were drilled on this base plate, which are used to fasten the plates to the test setup.

The channel shear connectors were welded to the base plate by making use of manual stick welding. A photo of a typical channel connector welded to the base plate is

indicated in Figure 2.6. After the welding process was completed, the perimeter of the channel shear connectors were covered with nylon to prevent the bond between filling material & steel plate as seen in Figure 2.6, and the concrete blocks were placed above the base plate with precise control of dimensions. The final operation was to fill the empty pockets with a proper filling material.

Figure 2.6. Channel shear connectors welded onto steel plate (a) The nylons covered at the bottom of shear pockets (b)

2.1.1. Test Parameters

The experimental part of the study included 20 push-out specimens with variable parameters. The channel height and width, as well as the type and strength of filling material were changed to investigate the performance of channel connectors under different conditions. The details of the specimens are given in Table 2.1. As shown in this table, European channel connectors with sizes that range between UPN65 to UPN140 were utilized. The channel connectors had two different widths of 50 mm and 75 mm to investigate the effect of width on the ultimate strength of connectors. Mortar and grout were selected as filling materials. Two different compressive strengths were considered for mortar filled specimens, which hereafter referred to as high strength mortar and low strength mortar.

Table 2.1. Specimen Properties for Push-Out Tests

Properties of Specimens				
Specimen #	Specimen Name	Channel section	Channel width (mm)	Filling Material
1	UPN65-M1-50	UPN65	50	High strength mortar
2	UPN80-M1-50	UPN80	50	High strength mortar
3	UPN100-M1-50	UPN100	50	High strength mortar
4	UPN120-M1-50	UPN120	50	High strength mortar
5	UPN140-M1-50	UPN140	50	High strength mortar
6	UPN65-M1-75	UPN65	75	High strength mortar
7	UPN80-M1-75	UPN80	75	High strength mortar
8	UPN100-M1-75	UPN100	75	High strength mortar
9	UPN120-M1-75	UPN120	75	High strength mortar
10	UPN140-M1-75	UPN140	75	High strength mortar
11	UPN65-M2-50	UPN65	50	Low strength mortar
12	UPN80-M2-50	UPN80	50	Low strength mortar
13	UPN100-M2-50	UPN100	50	Low strength mortar
14	UPN120-M2-50	UPN120	50	Low strength mortar
15	UPN140-M2-50	UPN140	50	Low strength mortar
16	UPN65-G-50	UPN65	50	Grout
17	UPN80-G-50	UPN80	50	Grout
18	UPN100-G-50	UPN100	50	Grout
19	UPN120-G-50	UPN120	50	Grout
20	UPN140-G-50	UPN140	50	Grout

2.1.2. Tensile Strength of Channel Shear Connectors

The material properties of channel shear connectors were determined by making use of coupon tests. Only one coupon was extracted from the web of channel connectors of each size and subjected to tension. The stress-strain response obtained from the tension tests are given in Figure 2.7. The geometrical and key material properties of each connector type are summarized in Table 2.2.

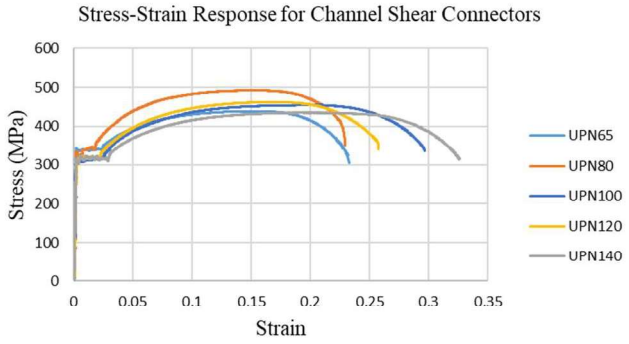

Figure 2.7. Tension Test Results of Channel Shear Connectors

Table 2.2. Geometric Properties and Tension Test Results of Channel Shear Connectors

Geometric and Material Properties of Channel Sections							
Channel Size	H (mm)	b_f (mm)	t_w (mm)	t_f (mm)	F_y (MPa)	F_u (MPa)	Maximum Elongation (%)
UPN65	65	42	5.5	7.5	338	439	23
UPN80	80	45	6.0	6.0	338	493	23
UPN100	100	50	6.0	8.5	309	457	30
UPN120	120	55	7.0	9.0	317	463	26
UPN140	140	60	7.0	10.0	315	435	33
H: Height		t_w: Web Thickness			F_y: Yield Strength		
		t_f: Flange Thickness			F_u: Tensile Strength		

2.1.3. Mix Proportion and Compressive Strengths of Filling Materials

As mentioned before high strength mortar, low strength mortar and grout (Sika-212) were used as filling materials. The nominal mix proportion and compressive strengths of these filling materials are given in Table 2.3 and Table 2.4, respectively. Compressive tests were conducted on both the 100x200 mm cylinder type and 50x50x50 mm and 150x150x150 mm cube type specimens and the results according to specimen dimensions are reported. In the following parts of the thesis the compressive strengths from cylinder specimens are used for discussion of results. The

compressive strengths for high strength mortar, low strength mortar and grout were determined as 40.74 MPa, 28.97 MPa and 42.47 MPa, respectively at the day of pushout testing. The low strength mortar was produced by increasing the water cement ratio of the high strength mortar mix and avoiding the use of ACE450 additive used for fluidity.

The filling materials were prepared and placed in shear pockets and the final form of the specimens are given in Figure 2.8 and Figure 2.9. The specimens used to determine compressive strength were kept at the same laboratory conditions as that of the push-out specimens.

Table 2.3. Nominal Mix Proportion of Filling Materials

High Strength Mortar		Low Strength Mortar		Grout	
Material:	Quantity (gr)	Material:	Quantity (gr)	Material:	Quantity (gr)
Cement (42.5):	500	Cement (42.5):	500	Grout	25000
Sand (0-4):	1350	Sand (0-4):	1350	Water	3250
Water	220	Water	300		
Additive (for fluidity)	5	Additive (for fluidity)	-		
w/c	0.44	w/c	0.6		

Table 2.4. The compressive capacities of filling materials in shear pockets

Compressive Strength of Filling Materials in Shear Pockets			
High Strength Mortar			
Time after casting	f_c cylinder (MPa)	f_c cube (50x50x50mm) (MPa)	f_c cube (150x150x150mm) (MPa)
Pushout test day (Day 21)	40.74	42.97	55.44
Day 28	43.29	45.93	57.80
Low Strength Mortar			
Time after casting	f_c cylinder (MPa)	f_c cube (50x50x50mm) (MPa)	f_c cube (150x150x150mm) (MPa)
Pushout test day (Day 21)	28.97	28.63	32.41
Day 28	29.29	27.83	34.48
Grout			
Time after casting	f_c cylinder (MPa)	f_c cube (50x50x50mm) (MPa)	f_c cube (150x150x150mm) (MPa)
Pushout test day (Day 21)	42.47	51.10	54.14
Day 28	44.50	50.67	54.72

Figure 2.8. Composite specimens with shear pockets filled with mortar

Figure 2.9. The cube and cylinder samples with precast specimens

2.1.4. Determining Elastic Modulus of Filling Materials

The filling material comes into direct contact with the channel connector and its mechanical properties, namely the strength and elastic modulus, are influential on the behavior of the shear connector. When concrete blocks are employed, the elastic modulus of concrete can be found from expressions that are available in concrete design codes. On the other hand, the elastic modulus of mortar and grout should be determined to be able to make a fair comparison between the modulus of elasticity of concrete and the one for the filling material. Compressive tests on cylindrical specimens were conducted to measure the stress-strain response of filling materials as seen in Figure 2.10 representatively. For each filling material, two tests were conducted and the average value was considered. In order to obtain the elastic modulus, 3 loading and unloading cycles were completed. The slope of the graphs which include second and third loading interval were taken as elastic modulus data where a representative behavior is indicated in Figure 2.11. The elastic modulus values of each filling material are reported in Table 2.5.

Figure 2.10. The MTS machine with cylinder sample during elasticity modulus test

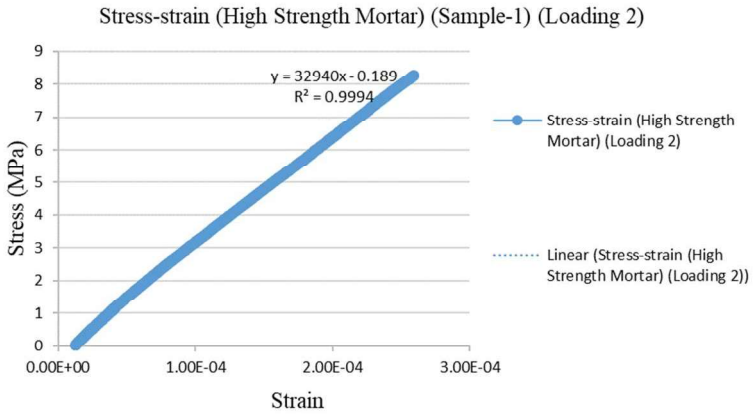

Figure 2.11. The stress-strain graph for second loading cycle of first cylindrical mortar sample

Table 2.5. Elastic modulus of filling materials

Elastic Modulus of Filling Materials	
Filling Material:	E (GPa):
High Strength Mortar	34.77
Low Strength Mortar	22.11
Grout	21.55

The elasticity modulus of concrete can be calculated with the equations supplied in TS500, ACI and Eurocode in Eqns 2.1, 2.2, and 2.3, respectively. The elasticity modulus of concrete of tests on conventional concrete specimens conducted by Baran&Topkaya (2012) and Topkaya&Yura (2004) obtained both from these code equations and elasticity tests in laboratory conditions can be seen in Table 2.6.

$$E_c = (3250 \times f_{ck}^{0.5}) + 14000 \qquad (2.1)$$

$$E_c = 4700 \times (f_c')^{0.5} \qquad (2.2)$$

$$E_c = 22000 \times (f_{cm} \div 10)^{0.3} \qquad (2.3)$$

where,

$f_{cm}=f_{ck}+8$ and f_{ck} is the cylindrical compressive strength of material

Table 2.6. Elasticity modulus of concrete in conventional specimens with respect to code equations

Elasticity modulus values					
Tests on conventional concrete specimens					
Specimens testes by Baran&Topkaya			Specimens tested by Topkaya&Yura		
	f_{ck} (MPa)	E_c (GPa)		f_{ck} (MPa)	E_c (GPa)
TS500	33	32.67	TS500	30.46	31.94
ACI	33	27.00	ACI	30.46	25.94
Eurocode	33	33.59	Eurocode	30.46	32.96
Average:	33	**31.09**	Average:	30.46	**30.28**
Test result	33	-	Test result	30.46	**28.91**

The results given in Table 2.6 indicate that the average elastic modulus from the three code equations are quite close to the measured one for the test conducted by Topkaya et al. (2004). The same procedure can be extended to estimate the modulus of elasticity of concrete used in tests of Baran and Topkaya (2012). By using this procedure, the modulus is estimated as 31.09 GPa and this value is close to the modulus of high strength mortar but higher than the modulus of low strength mortar and grout.

2.2. Push-out Test Setup

The test setup used for the push-out tests were similar to the one used by Baran and Topkaya (2012). The details of the test setup are shown in Figure 2.12 and Figure 2.13. The details of test specimen can also be investigated from Figure 2.14. In this test setup the test specimen with the base plate is placed over an HEA360 steel I-section. The base plate is bolted to the flange of HEA360 by making use of six M20 bolts. The load is applied to the test specimen by making use of a 600 kN capacity hydraulic jack. One end of the hydraulic jack was attached to a steel reaction block which was welded to the HEA360 beam.

A 1000 kN capacity load cell was placed at the end of the hydraulic jack to measure the applied loads. The rectangular steel plate with a 40 mm-thickness was placed between the load cell and specimen to distribute the load uniformly to the concrete surface and to minimize damage in front side of concrete. The steel plate was slotted on one side to allow contact of a ball bearing which transmits the horizontal load (Figure 2.15 and Figure 2.16).

In this type of a test setup the horizontal jack axis does not coincide with the weld group used to fasten the channel connector. The eccentricity of load application results in uplift of the concrete slab and produces tensile loading on the connector. In order to simulate pure shear conditions a clamping mechanism was used in the test setup. This mechanism consists of two UPN120 sections positioned back-to-back and connected to each other by welded steel plates. Two built-up UPN sections were used one placed above the concrete slab and the other placed below the bottom flange of the HEA360 section. Two steel rods with 36 mm diameter were used to clamp the two built-up sections together. In order to eliminate friction being developed between the built-up section and the concrete slab a roller mechanism was developed and used. As seen in Figure 2.17 and Figure 2.18 this mechanism employs two steel plates and several steel ball bearings that are placed in between the plates. This mechanism was greased to reduce the amount of friction and allowed for free movement of the

concrete block even after the application of a high clamping force. Two LVDTs were placed at the unloaded ends of the specimen to monitor the amount of slip during testing.

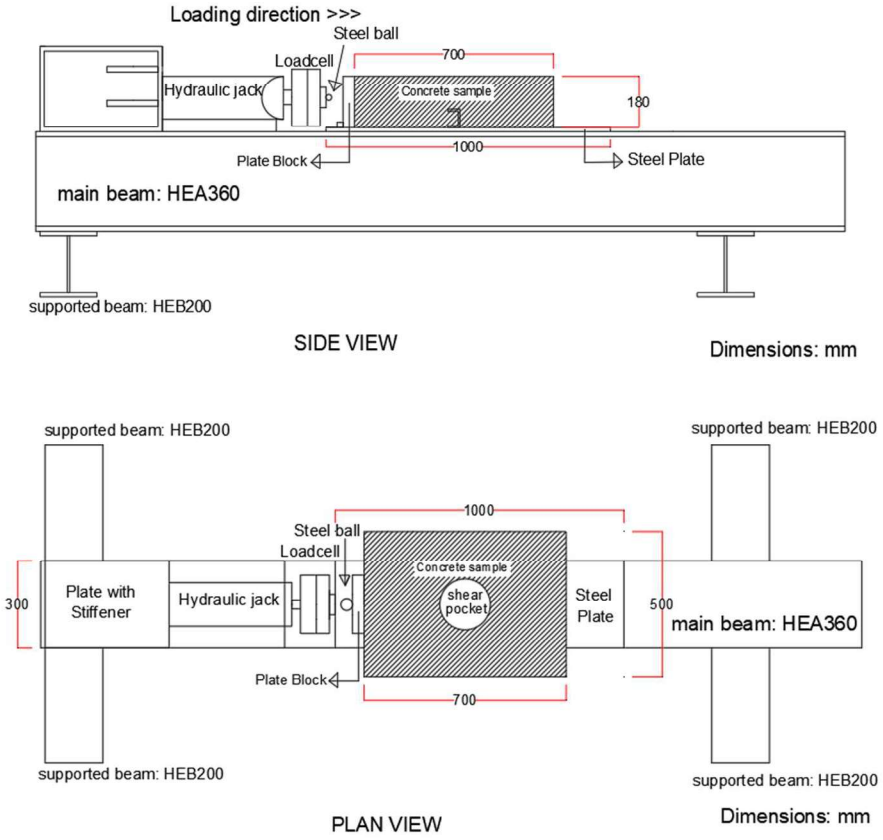

Figure 2.12. Pushout test setup (a) Side View (b) Plan view

Figure 2.13. The general view of push-out test setup

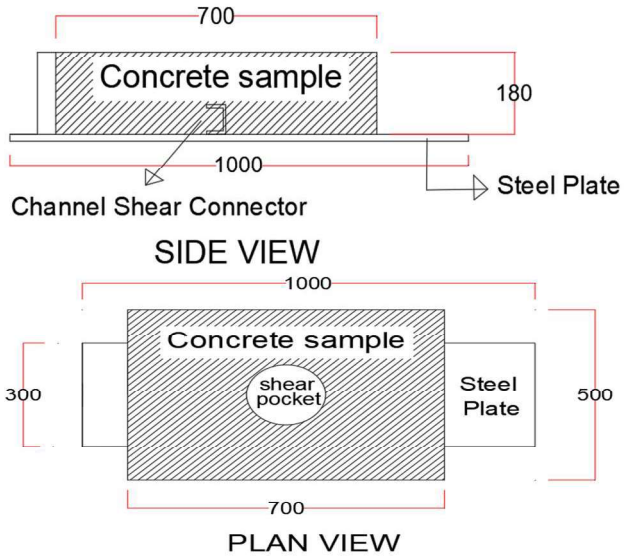

Figure 2.14. The details of pushout test specimen (a)Side View (b) Plan View

Figure 2.15. Load cell and its connection with push-out specimen

Figure 2.16. The slotted rectangular steel plate

Figure 2.17. The interior view between rubber plates

Figure 2.18. The clamping mechanism placed on the rubber plates

2.3. Test Results

The test results of push-out tests are presented in terms of failure mode, load-slip response, stiffness of specimens, and plastic hinge locations in the following sections.

2.3.1. Failure Mode

The failure of channel connectors occurred due to fracture of channel shear connector near the fillet between the web and the flange in all of the specimens. It was an expected behavior since the same failure type was observed in the study of Baran&Topkaya (2012) during push-out tests of cast-in-situ concrete-steel composite specimens with channel shear connectors. Therefore, it can be said that channel connectors embedded in shear pockets filled with either mortar or grout fail in the

same manner while having different load slip behaviors as mentioned in the following sections.

Moreover, cracking was observed in the surface of concrete blocks, especially around the shear pockets. After the completion of loading tests, the channel shear connectors embedded in shear pocket were taken out with the help of concrete breaker to inspect the deformed shape of them in detail and to measure the plastic hinge locations. Additionally, some deformation patterns on the surface of concrete deck were marked with pen to follow the deformation pattern arisen from loading as seen in Figure 2.19 and the back side of blocks can also be seen in Figure 2.20. The deformation pattern concentrates around and on the surface of filling materials.

The deformed channel shear connectors can be seen in Figure 2.21 and Figure 2.22. In Figure 2.21, the channels in the front face are the channels which have a width of 50 mm and surrounded with high strength mortar, and the channels in the back side are the channels which have a width of 75 mm and surrounded with high strength mortar. Additionally, in Figure 2.22, all of the channels have a width of 50 mm, but the channels in the front row were in the shear pockets of low strength mortar while the others in the back row were in the shear pockets of grout. The typical deformation pattern is bending deformation at the lower part of the web can be seen in all of the photos clearly. The channel shear connectors in these figures were placed upside down one by one and the flanges absent in these figures were the welded portion remained on the steel plate. Moreover, an example to the precast concrete block is added in Figure 2.23 to understand that the filling material and concrete worked together.

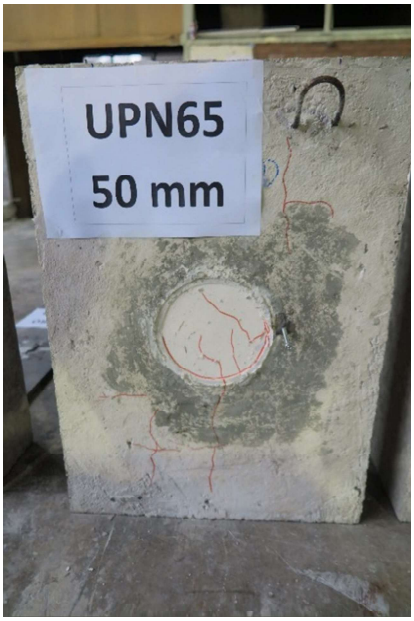

Figure 2.19. The precast concrete blocks after tests with marks on deformation patterns

Figure 2.20. The back side of the precast concrete blocks after

Figure 2.21. The deformation pattern of channel shear connectors (Channels are shown upside down.)

Figure 2.22. The deformation pattern of channel shear connectors (Channels are shown upside down.)

Figure 2.23. An example of concrete damage around channel shear connectors

2.3.2. Load-Slip Response

In this section the load slip response obtained from the push-out tests are presented and compared with the response obtained using conventional concrete specimens. The

maximum load and slip values obtained at the end of push-out tests are given in Table 2.7 and Table 2.8 for precast concrete specimens tested in this study and conventional concrete specimens tested by Baran&Topkaya, respectively.

Table 2.7. Push-out test results of precast specimens

Precast Specimens			
Specimen #	Specimen Name	Measured max. capacity (kN)	Measured Max. Slip (mm)
1	UPN65-M1-50	301.8	13.74
2	UPN80-M1-50	328.8	15.57
3	UPN100-M1-50	340.0	18.07
4	UPN120-M1-50	372.8	18.85
5	UPN140-M1-50	307.1	15.50
6	UPN65-M1-75	413.9	17.83
7	UPN80-M1-75	390.8	16.37
8	UPN100-M1-75	416.7	17.90
9	UPN120-M1-75	473.3	23.81
10	UPN140-M1-75	437.0	22.03
11	UPN65-M2-50	254.6	19.47
12	UPN80-M2-50	263.5	19.50
13	UPN100-M2-50	297.4	21.63
14	UPN120-M2-50	340.5	24.44
15	UPN140-M2-50	353.2	27.88
16	UPN65-G-50	319.0	15.72
17	UPN80-G-50	334.8	15.61
18	UPN100-G-50	352.4	21.57
19	UPN120-G-50	368.5	22.72
20	UPN140-G-50	395.6	21.41
Capacity of Filling Materials used in Shear Pockets of Precast Deck-Steel Composite Specimens			
Filling Material:		**fc cylinder at test day (MPa):**	**Ec (GPa):**
Mortar (w/c=0.44)		40.74	34.77
Mortar (w/c=0.6)		28.97	22.11
Grout		42.47	21.55

Table 2.8. Push-out test results of conventional concrete specimens (Study of Baran&Topkaya)

Conventional Specimens			
Specimen #	Specimen Name	Measured max. capacity (kN)	Measured Max. Slip (mm)
1	UPN65-50	218.4	11.00
2	UPN80-50	252.6	23.34
3	UPN100-50	291.6	23.79
4	UPN120-50	293.1	21.27
5	UPN140-50	302.6	21.63
6	UPN65-75	292.6	16.47
7	UPN80-75	310.4	26.68
8	UPN100-75	345.1	30.00
9	UPN120-75	385.2	31.99
10	UPN140-75	401.3	28.57

The comparison of load and deformation behavior of channel shear connectors between this study and study of Baran and Topkaya (2012) are provided in this section. The study of Baran and Topkaya (2012) represents the behavior of channel shear connector embedded in cast-in-situ concrete while the study of this thesis indicates the behavior of channel shear connectors in shear pocket filled with mortar or grout to utilize a precast deck. Therefore, it means that this comparison provides insight into the influence of choosing precast deck instead of cast-in-situ concrete in terms of structural parameters.

The comparison between the load-slip behavior of precast and conventional composite systems can be investigated from Figure 2.24 to Figure 2.33 for channel sizes of UPN65 to UPN140 in ascending order. In general, precast deck-steel composite specimens gave higher maximum load capacities than others for the same channel size while the same comment is not valid for deformation capacities, but still, the 6 mm limit to be ductile in accordance with Eurocode was fulfilled for each precast specimen.

The compressive capacity of filling material placed around connectors to create shear pocket directly influences to the load capacity of connector. However, UPN140 section in high strength mortar has lower strength than the same section in low strength mortar, and it can be interpreted as an error due to test conditions.

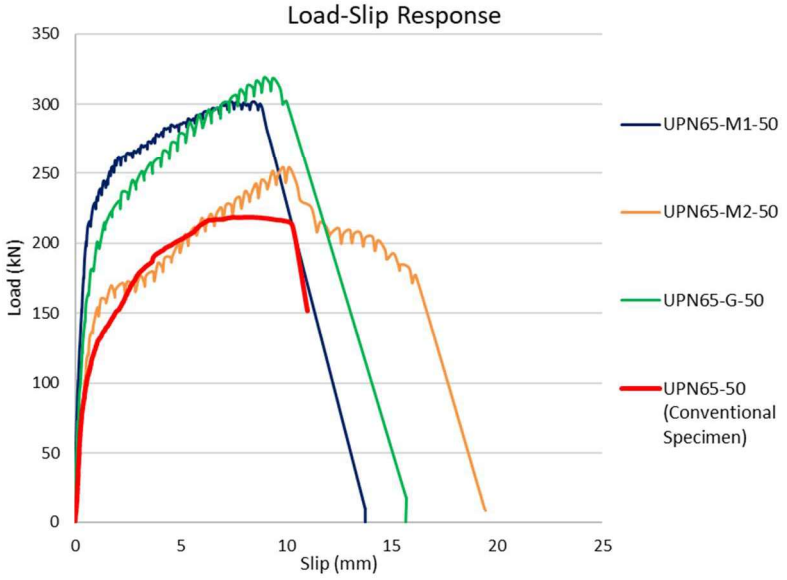

Figure 2.24. Load-slip behavior to compare precast and conventional specimens (UPN65-50)

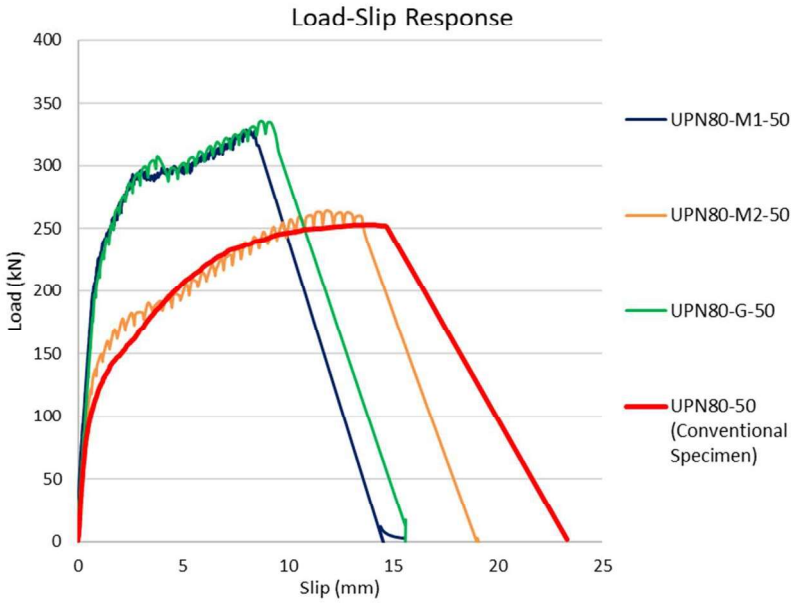

Figure 2.25. Load-slip behavior to compare precast and conventional specimens (UPN80-50)

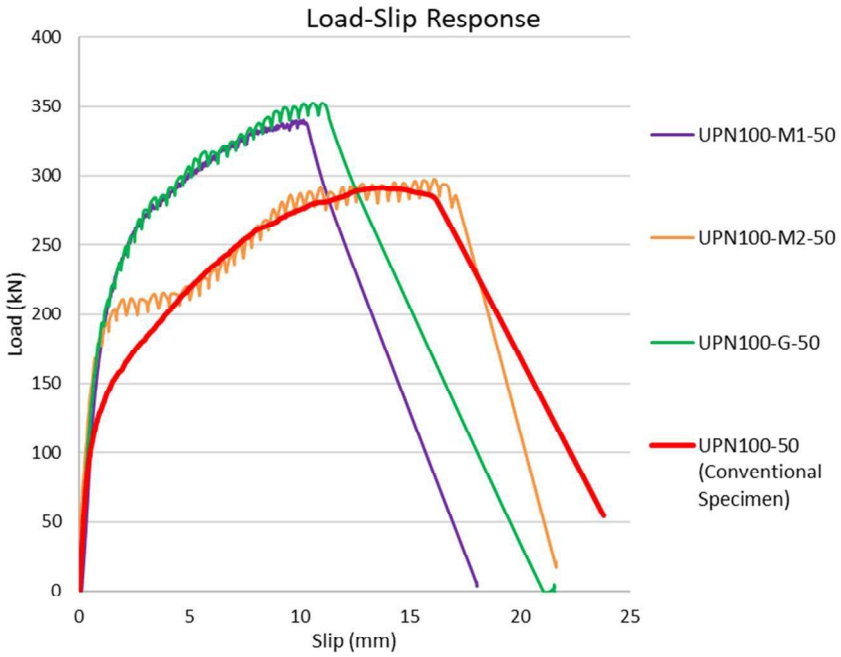

Figure 2.26. Load-slip behavior to compare precast and conventional specimens (UPN100-50)

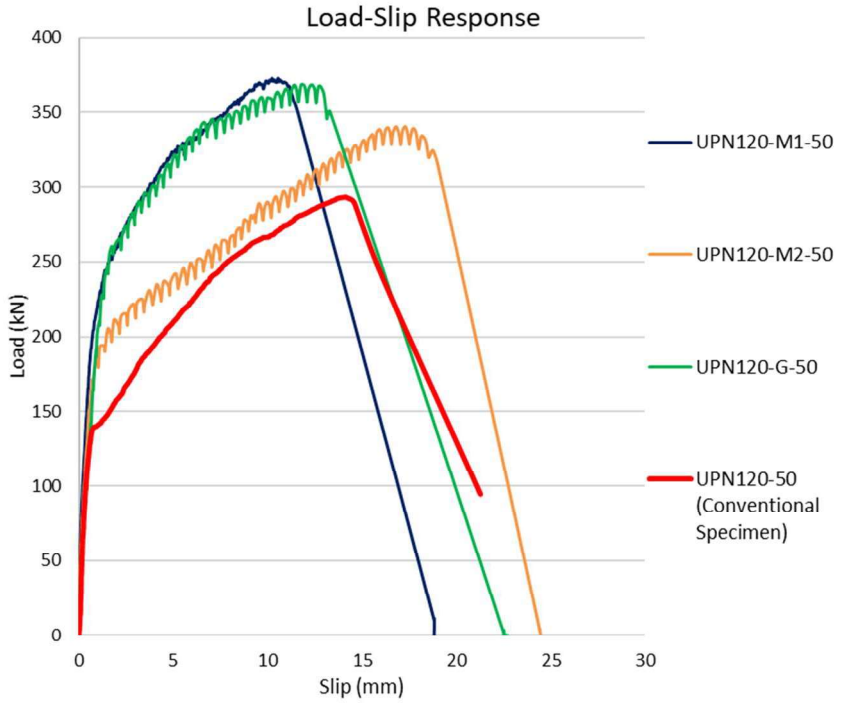

Figure 2.27. Load-slip behavior to compare precast and conventional specimens (UPN120-50)

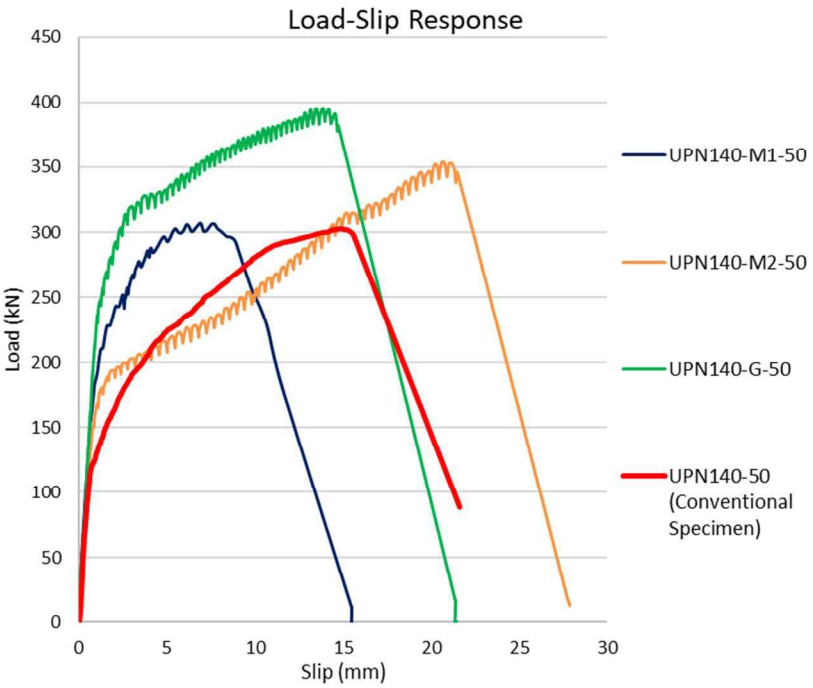

Figure 2.28. Load-slip behavior to compare precast and conventional specimens (UPN140-50)

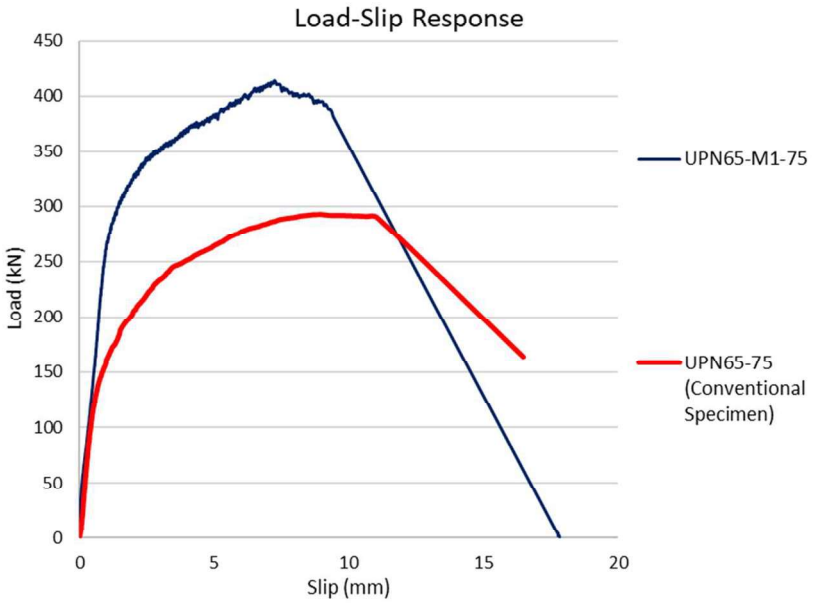

Figure 2.29. Load-slip behavior to compare precast and conventional specimens (UPN65-75)

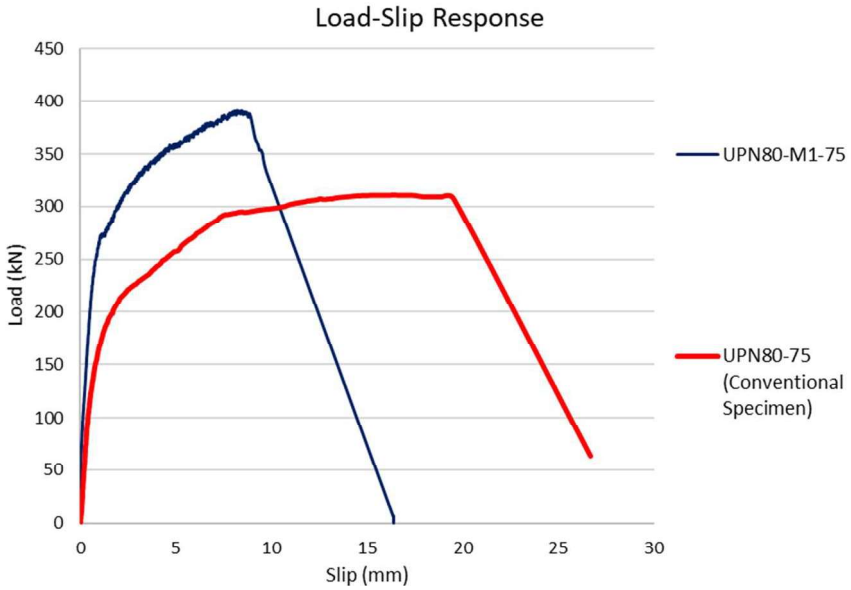

Figure 2.30. Load-slip behavior to compare precast and conventional specimens (UPN80-75)

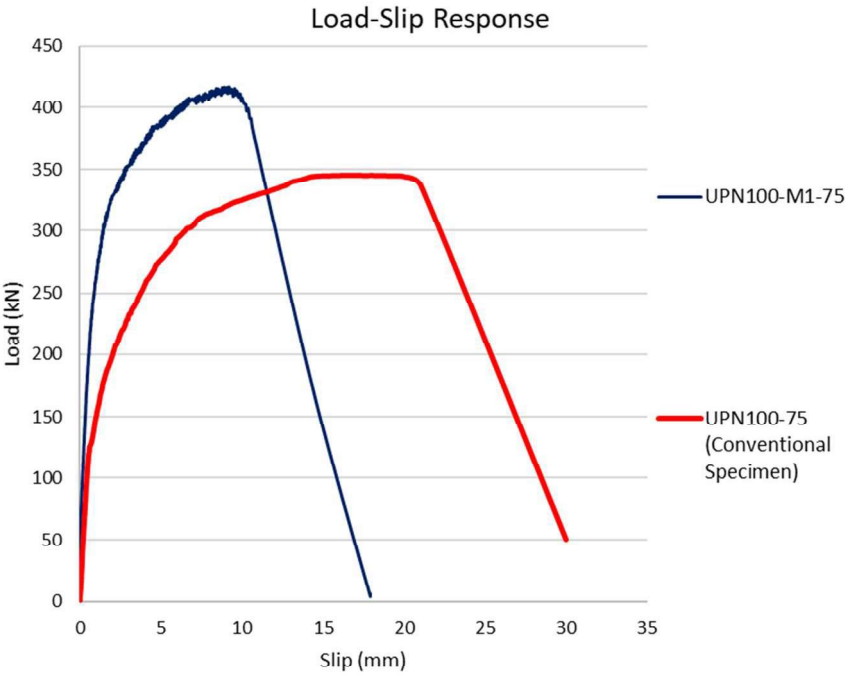

Figure 2.31. Load-slip behavior to compare precast and conventional specimens (UPN100-75)

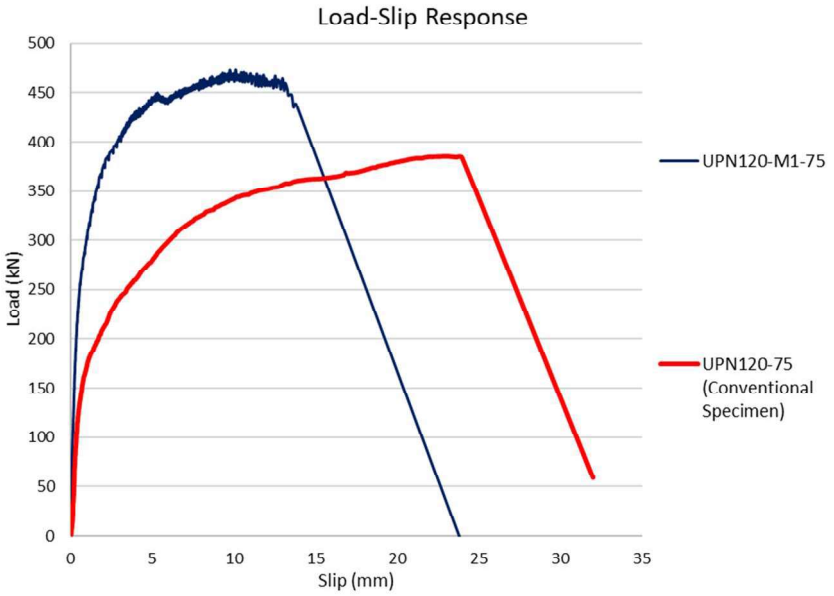

Figure 2.32. Load-slip behavior to compare precast and conventional specimens (UPN120-75)

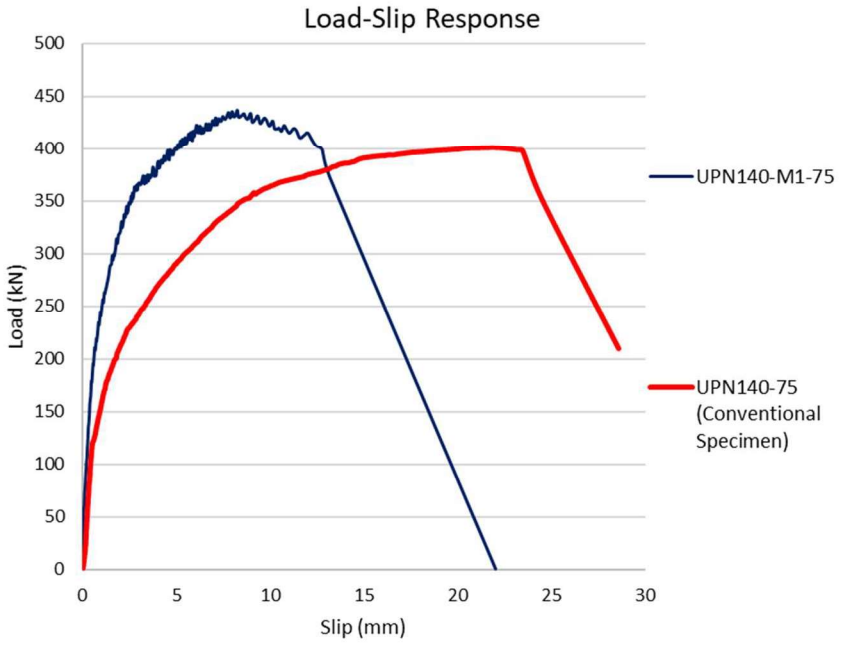

Figure 2.33. Load-slip behavior to compare precast and conventional specimens (UPN140-75)

The comparison of channel sizes for the same channel width and filling material can be seen in Figure 2.34 and Figure 2.35. These figures show that as the channel section gets larger, higher load and slip capacity can be reached.

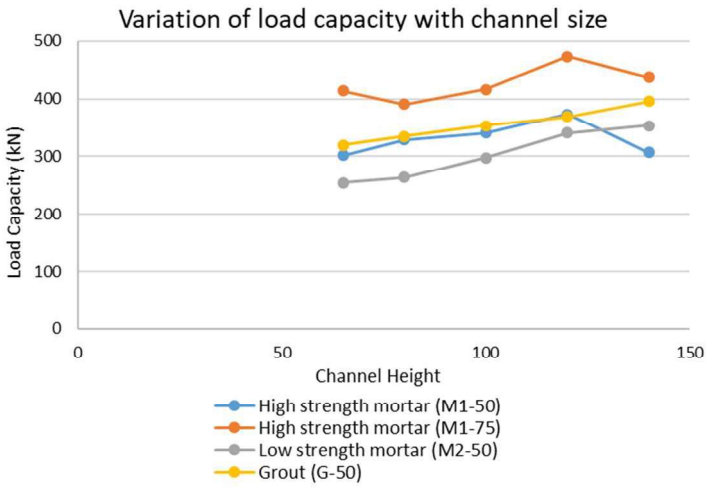

Figure 2.34. Effect of channel size on load capacity

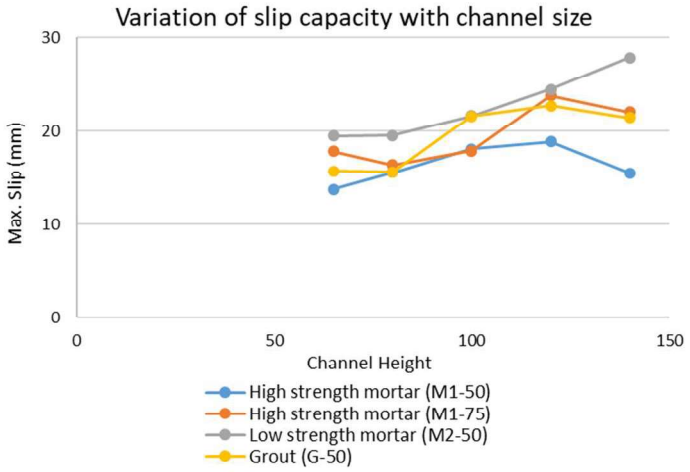

Figure 2.35. Effect of channel size on slip capacity

The effect of channel length on the load and deformation capacity is indicated in Figure 2.36 and Figure 2.37, respectively. As shown in this figure the capacity increases with an increase in the length of the channel connector.

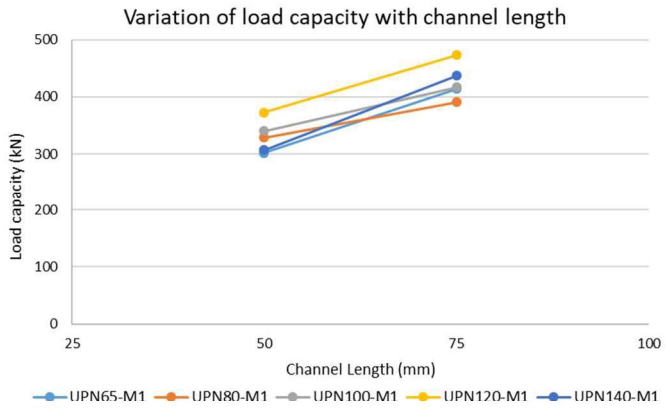

Figure 2.36. Effect of channel length on load capacity

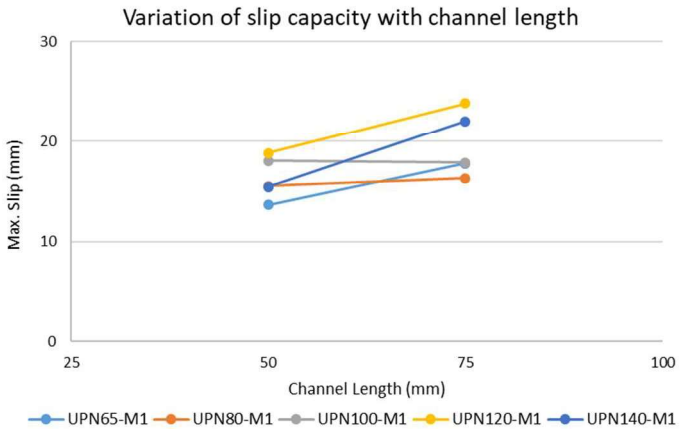

Figure 2.37. Effect of channel length on slip capacity

As seen in these test results, load capacity and ductility of channel connectors increase with an increase in the channel size, channel length and compressive capacity of filling material.

2.3.3. Stiffness Calculation of Channel Shear Connectors

The stiffness values of each specimen calculated at fixed deformation values can be seen in Table 2.9. These values were calculated by taking the tangent stiffness at the deformation points of 0.3 and 0.8 mm, and a representative load-slip graph is given in Figure 2.38. When the results are investigated in terms of filling materials, it can be

stated that the increase in rigidity is in general directly proportional with the compressive capacity of filling material. Moreover, the channel width often increases the stiffness clearly.

Table 2.9. Tangent stiffness values of precast specimens

# of Specimen	Specimen Name	k (Tangent Stiffness) (kN/mm)
1	UPN65-M1-50	138.29
2	UPN80-M1-50	190.65
3	UPN100-M1-50	221.24
4	UPN120-M1-50	167.25
5	UPN140-M1-50	163.24
6	UPN65-M1-75	260.45
7	UPN80-M1-75	202.61
8	UPN100-M1-75	195.06
9	UPN120-M1-75	177.29
10	UPN140-M1-75	185.59
11	UPN65-M2-50	116.42
12	UPN80-M2-50	111.57
13	UPN100-M2-50	132.94
14	UPN120-M2-50	145.86
15	UPN140-M2-50	148.15
16	UPN65-G-50	112.75
17	UPN80-G-50	203.57
18	UPN100-G-50	165.97
19	UPN120-G-50	191.04
20	UPN140-G-50	233.03

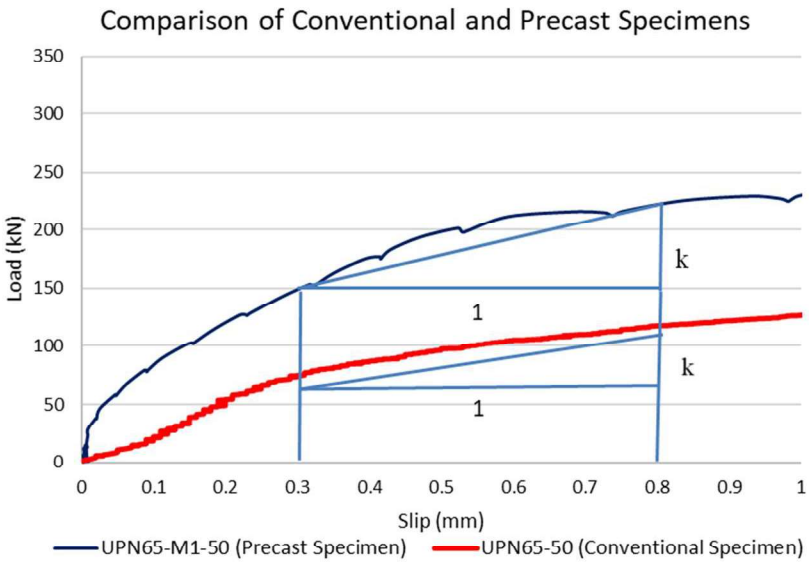

Figure 2.38. The deformation interval of the tangent stiffness calculation

The influence of selection of precast or conventional specimens on stiffness values can also be analyzed from Figure 2.39, Figure 2.40, Figure 2.41, and Figure 2.42 for each filling materials tested in precast decks and conventional concrete specimens.

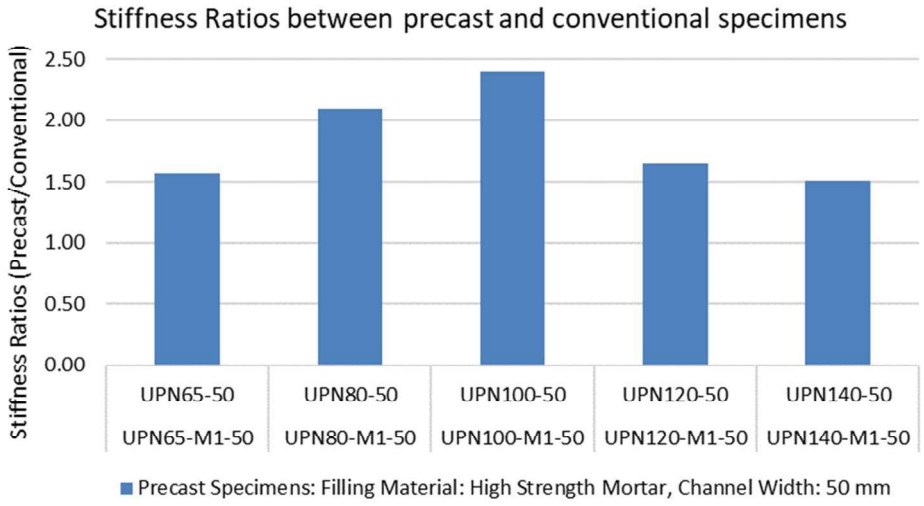

Figure 2.39. Stiffness comparison between precast (M1-50) and conventional specimens

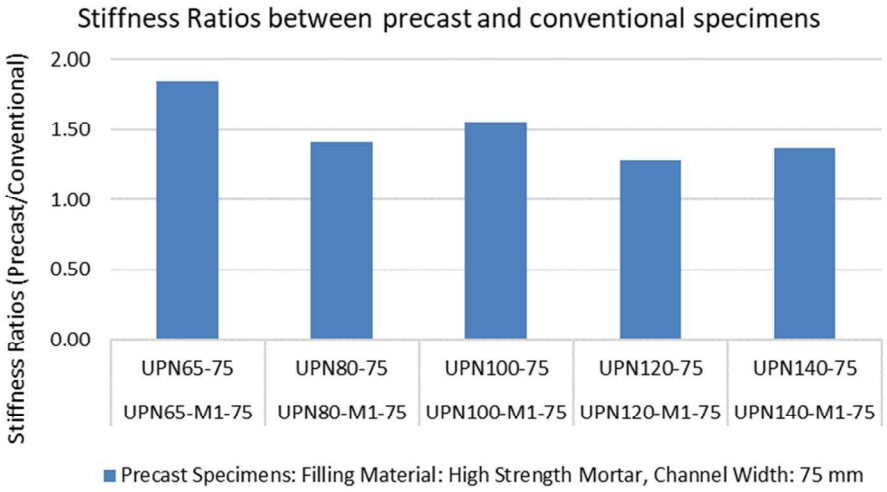

Figure 2.40. Stiffness comparison between precast (M1-75) and conventional specimens

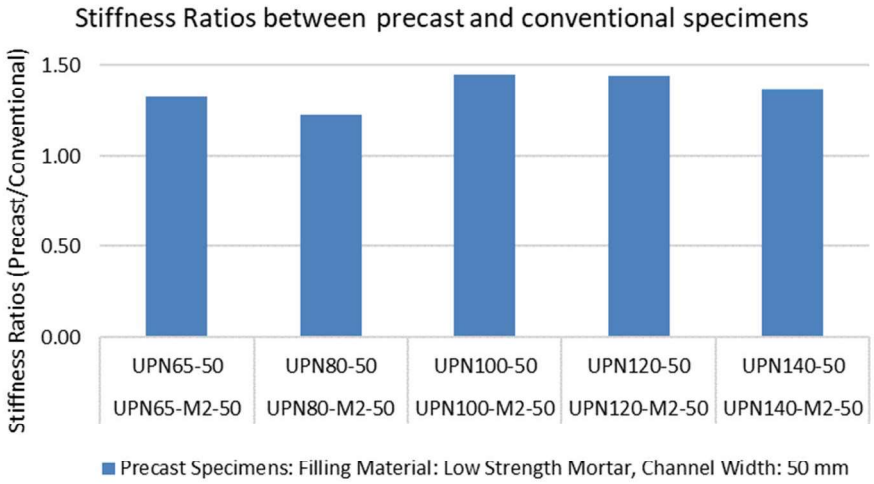

Figure 2.41. Stiffness comparison between precast (M2-50) and conventional specimens

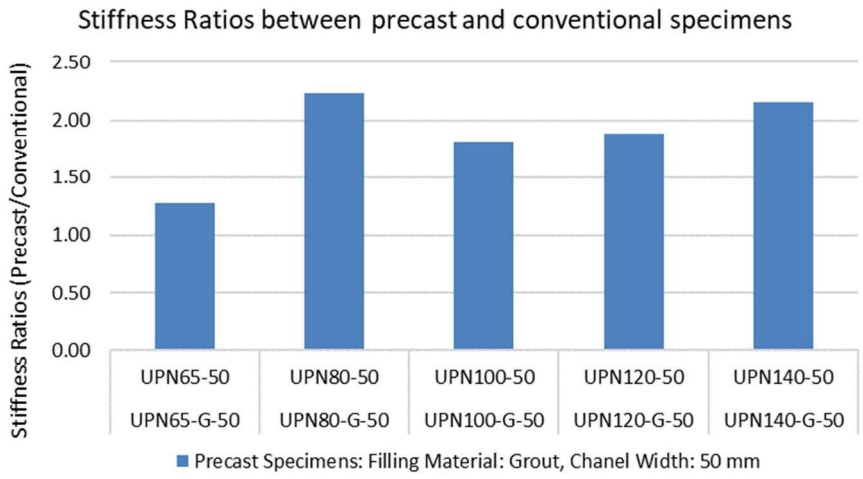

Figure 2.42. Stiffness comparison between precast (G-50) and conventional specimens

If a comparison between this study and the study of Baran&Topkaya (2012) in terms of stiffness is conducted, results clearly indicate that channel connectors in precast deck systems are stiffer than the ones used in conventional systems. Moreover, this fact is valid for not only for grout or high strength mortar filled specimens, but also low strength mortar filled specimens.

2.3.4. Measured Fracture and Plastic Hinge Locations

Two plastic hinges form on channel shear connectors based on the failure shape. One of them occurred near the fillet between the web and the flange and the other one occurred at the lower part of the web. The plastic hinge locations can be examined in Figure 2.43 which is from the study of Baran&Topkaya (2012) since the failure pattern based on h_1 and h_2 was the same with the channels used in the study of these researchers. As seen from this figure, h_1 is the channel height from bottom to the inflection point and h_2 is the channel height included the channel part on the steel plates after rupture. The fracture and plastic hinge values for the channel shear connectors in this study can be found in Table 2.10. The ratios of measured hinge locations of precast and cast-in-situ systems can be found in Table 2.11. As seen from

these ratios, the plastic hinge distances between these two types of specimens are not too different from each other between the same channel sizes except UPN100. These values were necessary to develop an empirical equation which gives connector strength in steel-concrete composite beams, i.e. load capacity of these specimens as explained in the following section.

The hinge locations from the two test series should be compared because the connector strength is dependent on the hinge locations as determined by Baran and Topkaya (2012). The average values reported in Table 2.11 indicate that there are no significant differences in hinge locations for the conventional specimens and the ones that utilize a filling material.

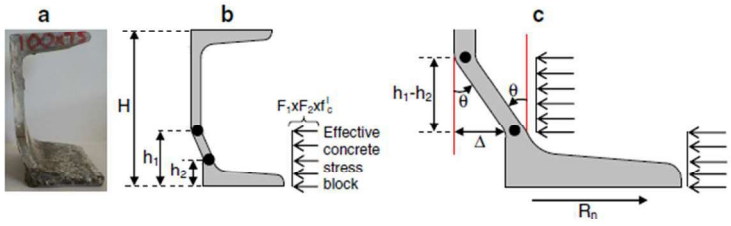

Figure 2.43. Typical failure mechanism of channel shear connectors in composite systems (Baran & Topkaya, 2012)

Table 2.10. Measured fracture and plastic hinge locations of precast deck specimens

Specimen	H (mm)	h_2 (mm)	h_1 (mm)	$(h_1-h_2)/H$	$(h_2+(h_1-h_2)/2)/H$
UPN65-M1-50	65	8.00	28.50	0.32	0.28
UPN80-M1-50	80	9.00	27.50	0.28	0.28
UPN100-M1-50	100	8.00	31.50	0.29	0.25
UPN120-M1-50	120	9.00	31.50	0.28	0.25
UPN140-M1-50	140	7.00	30.50	0.24	0.19
UPN65-M1-75	65	9.00	33.50	0.25	0.21
UPN80-M1-75	80	12.00	36.50	0.20	0.20
UPN100-M1-75	100	11.00	43.00	0.27	0.23
UPN120-M1-75	120	13.00	39.00	0.19	0.19
UPN140-M1-75	140	13.00	35.00	0.16	0.17
			Average:	0.25	0.22
			St. Dev. :	0.05	0.04
Specimen	H (mm)	h_2 (mm)	h_1 (mm)	(h1-h2)/H	(h2+(h1-h2)/2)/H
UPN65-M2-50	65	8.50	27.50	0.29	0.28
UPN80-M2-50	80	9.60	35.00	0.32	0.28
UPN100-M2-50	100	9.60	38.50	0.29	0.24
UPN120-M2-50	120	13.00	49.00	0.30	0.26
UPN140-M2-50	140	15.00	58.00	0.31	0.26
			Average:	0.30	0.26
			St. Dev. :	0.01	0.02
Specimen	H (mm)	h_2 (mm)	h_1 (mm)	(h1-h2)/H	(h2+(h1-h2)/2)/H
UPN65-G-50	65	7.50	24.50	0.26	0.25
UPN80-G-50	80	10.00	29.75	0.25	0.25
UPN100-G-50	100	9.90	31.50	0.22	0.21
UPN120-G-50	120	11.00	37.50	0.22	0.20
UPN140-G-50	140	12.50	42.50	0.21	0.20
			Average:	0.23	0.22
			St. Dev. :	0.02	0.03

Table 2.11. Relation between measured hinge locations of precast and cast-in-situ systems

Relation between hinge locations of conventional and precast specimen						
			Conventional Specimen / Precast Specimen:			
Conventional specimen	Precast Specimen	H (mm)	Ratio of h2	Ratio of h1	Ratio of (h1-h2)/H	Ratio of (h2+(h1-h2)/2)/H
UPN65-50	UPN65-M1-50	65	1.00	0.81	0.73	0.85
UPN80-50	UPN80-M1-50	80	1.13	0.95	0.89	0.99
UPN100-50	UPN100-M1-50	100	1.86	1.21	1.02	1.33
UPN120-50	UPN120-M1-50	120	1.00	1.18	1.27	1.13
UPN140-50	UPN140-M1-50	140	1.00	1.28	1.42	1.21
UPN65-75	UPN65-M1-75	65	0.89	0.91	0.92	0.90
UPN80-75	UPN80-M1-75	80	1.11	1.02	0.98	1.04
UPN100-75	UPN100-M1-75	100	1.44	1.13	1.02	1.20
UPN120-75	UPN120-M1-75	120	1.18	1.12	1.09	1.13
UPN140-75	UPN140-M1-75	140	1.08	1.63	1.95	1.48
Average:			1.17	1.12	1.13	1.13
UPN65-50	UPN65-M2-50	65	0.94	0.84	0.79	0.86
UPN80-50	UPN80-M2-50	80	0.94	0.86	0.83	0.87
UPN100-50	UPN100-M2-50	100	1.35	0.96	0.83	1.04
UPN120-50	UPN120-M2-50	120	0.92	0.88	0.86	0.89
UPN140-50	UPN140-M2-50	140	0.87	0.86	0.86	0.86
Average:			1.00	0.88	0.83	0.91
UPN65-50	UPN65-G-50	65	1.07	0.94	0.88	0.97
UPN80-50	UPN80-G-50	80	0.90	1.01	1.06	0.98
UPN100-50	UPN100-G-50	100	1.31	1.17	1.11	1.21
UPN120-50	UPN120-G-50	120	1.09	1.15	1.17	1.13
UPN140-50	UPN140-G-50	140	1.04	1.18	1.23	1.15
Average:			1.08	1.09	1.09	1.09

2.3.4.1. Connector Strength Prediction

The capacity formula derived from Baran&Topkaya (2012) can be seen in Eq. 1.4. This formula was derived for the working principle of cast-in-situ deck-steel composite systems, so the suitability this formulation to precast deck-steel composite system is also investigated here. The calculated connector strength for precast

specimens in push-out tests can be seen in Table 2.12. The ratio between predicted and measured load capacities for each filling material can be examined in Figure 2.44.

Table 2.12. Predicted and measured load capacities of specimens

Channel shear connectors in Precast deck specimens			
Specimen	Predicted capacity Rn (kN) (factor:0.25)	Measured capacity Rn (kN)	Ratio of Predicted-to-measured load capacity
UPN65-M1-50	255.74	301.84	0.85
UPN80-M1-50	293.31	328.76	0.89
UPN100-M1-50	324.55	339.98	0.95
UPN120-M1-50	351.65	372.84	0.94
UPN140-M1-50	360.29	307.05	1.17
UPN65-M1-75	350.06	413.92	0.85
UPN80-M1-75	401.31	390.81	1.03
UPN100-M1-75	442.90	416.68	1.06
UPN120-M1-75	480.04	473.33	1.01
UPN140-M1-75	491.25	437.04	1.12
Average:			0.99
Standard deviation:			0.11
UPN65-M2-50	187.76	254.57	0.74
UPN80-M2-50	214.98	263.46	0.82
UPN100-M2-50	235.54	297.43	0.79
UPN120-M2-50	255.52	340.47	0.75
UPN140-M2-50	260.60	353.22	0.74
Average:			0.77
Standard deviation:			0.04
UPN65-G-50	265.73	319.01	0.83
UPN80-G-50	304.82	334.83	0.91
UPN100-G-50	337.63	352.42	0.96
UPN120-G-50	365.78	368.55	0.99
UPN140-G-50	374.95	395.59	0.95
Average:			0.93
Standard deviation:			0.06
For all specimens:			
Average:			0.92
Standard deviation:			0.13

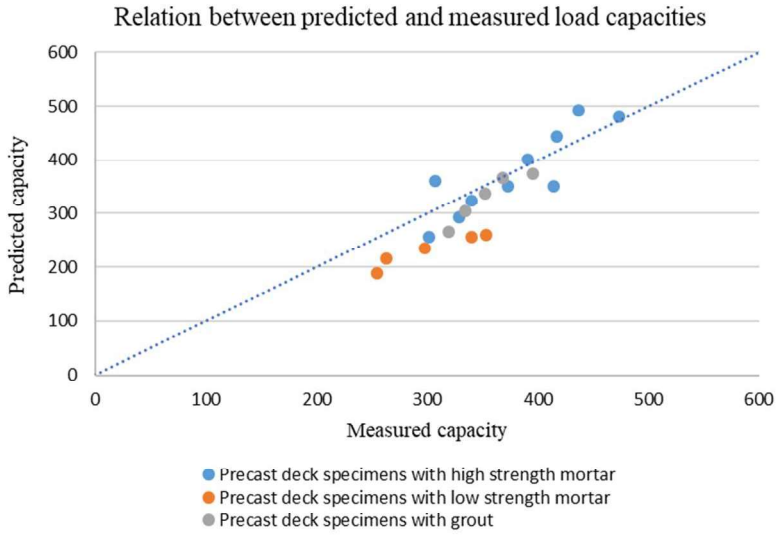

Figure 2.44. Relationship between predicted and measured capacities

The compressive strength of concrete specimen used in conventional specimens was between 31.8 and 34.5 MPa, so this formulation was derived for this interval. As seen in these graphs, the capacity formulation derived by Baran&Topkaya (2012) is also suitable with precast deck systems with high strength mortar as filling material, but the other specimens with low-strength mortar and grout as filling material gave more conservative results when compared with measured capacity values.

Compressive capacity of high strength mortar, low strength mortar and grout are 40.74, 28.97, and 42.47 MPa, respectively, so it means that this equation is suitable with higher strength values, as well. Moreover, the elasticity modulus values of concrete in conventional specimens, high strength mortar, low strength mortar and grout were 31, 34, 22 and 21 GPa, respectively, and it is clearly seen that the concrete in conventional deck specimens and high strength mortar has similar elasticity modulus values, so elasticity modulus values are effective on the suitability of this strength equation.

Therefore, it is determined as the empirical equation for connector strength prediction derived from Baran&Topkaya (2012) can be conservatively used for precast deck-steel composite specimens.

CHAPTER 3

BEAM TESTS

This chapter describes the second phase of the experimental study which consisted of beam tests. These tests were conducted at the Structural Mechanics Laboratory of the Department of Civil Engineering to examine the behavior of precast deck-steel composite beams. The composite action of these composite beams was formed with channel shear connectors embedded in shear pockets filled with mortar or grout.

3.1. Test Specimen Design

The beam specimens were prepared with the same corrugated pipes used in push-out tests as seen in Figure 3.1. The mesh reinforcements were terminated in the pipe area. The precast concrete decks after ready-mix concrete casting can be seen in Figure 3.2. After concrete hardened, the corrugated pipes were removed with blowtorch using the same procedure applied during preparation of push-out specimens. The channel shear connectors were cut and welded onto the steel beam. Steel plates with a thick of 3 mm were welded on both sides of beam top flange at channel shear locations in order to avoid leakage of infill material as seen in Figure 3.3. The precast decks were placed onto the steel beam with channel shear connectors welded on it. The pockets in decks and channels are indicated in Figure 3.4. At the end of these steps, these shear pockets were filled with filling materials to develop composite action between concrete block and steel beam.

Figure 3.1. The corrugated pipes placed in formworks of beam specimens

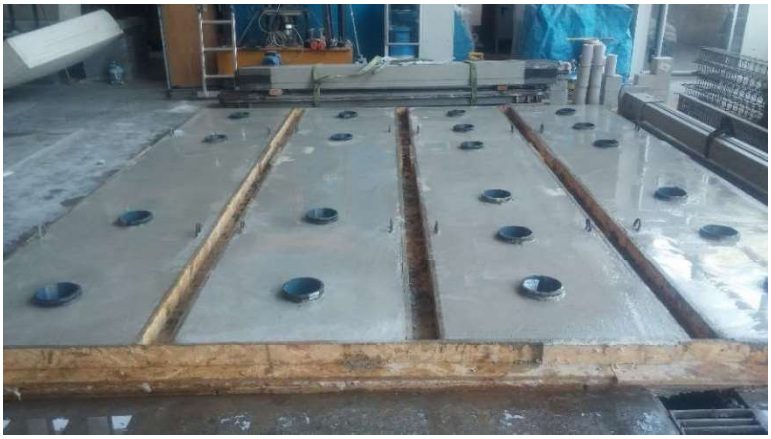

Figure 3.2. The precast deck specimens

Figure 3.3. The channel shear connectors welded onto steel section with plates in two sides

Figure 3.4. The shear pocket with channel shear connector

3.1.1. Test Parameters

The experimental part of the study included 4 beam specimens with variable parameters which are degree of composite action, type and capacity of filling materials, and channel width. The channel shear connector used in each composite beam specimen was UPN65, and the details of the specimens such as distance between shear connectors and degree of composite action are given in Table 3.1. The first and second beam had 4 connectors with a degree of composite action of 0.53 and 0.56, respectively. The third and fourth ones had 6 connectors with a degree of composite action of 0.66 and 1.08, respectively. The shear pockets of first and last composite beams were filled with high strength mortar which was used in push-out tests. The shear pocket of second and third composite beams were filled with grout and low strength mortar which were used in push-out tests, as well.

The details of first and second beam specimens, and third and fourth beam specimens can be investigated in Figure 3.5 and Figure 3.6, respectively. The front view of all of specimens can also be seen in Figure 3.7.

While casting of concrete decks, cylinder samples with a diameter of 100 mm and height of 200 mm were also taken to determine the strength of the mixture. The cylindrical compressive capacity of concrete slab was 32.67 MPa at 28^{th} day after

casting. The cylindrical compressive capacity of concrete slab for each specimen at test day can also be seen in Table 3.1.

The calculation of degree of composite action was based on the study of Baran&Topkaya (2014). The connector strength capacities were taken from the push-out test results. Then, the degree of composite action of each specimen was predicted by using the yield strength of IPE240 steel section and total connector strength. An average yield strength of 293.9 MPa was used in calculations. The formulation of degree of composite action can be seen in Equation 3.1.

$$\text{Degree of Composite Action} = \frac{\sum Q_n}{\min(A_s F_y, 0.85 f_c' A_c)} \qquad (3.1)$$

where,

F_y: yield strength of steel section

A_s: Area of steel section

f'_c: compressive strength of concrete

A_c: Area of concrete

Q_n: Connector strength

Table 3.1. Properties of specimens

Specimen #	Specimen name	Filling Material	Connector #	s_1 (cm)	s_2 (cm)	f_c' (MPa)	$\Sigma Q_n / F_y A_s$
1	UPN65-M1-50-C2	HSM	2	82.5	165	32.67	0.53
2	UPN65-G-50-C2	G	2	82.5	165	31.56	0.56
3	UPN65-M2-50-C3	LSM	3	55	110	32.54	0.66
4	UPN65-M1-75-C3	HSM	3	55	110	30.99	1.08

s_1, s_2: Shear connector spacing — HSM: High Strength Mortar

f_c' : Concrete compressive strength — LSM: Low Strength Mortar

Connector #: Connector number per shear span — G: Grout

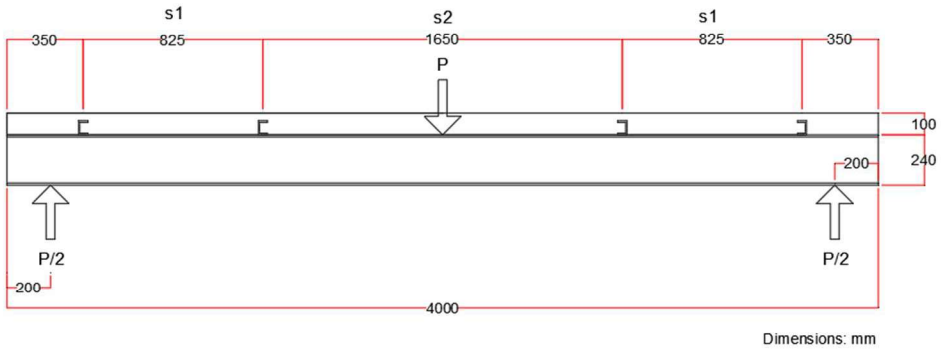

Figure 3.5. Details of test specimen 1 and 2 (side view)

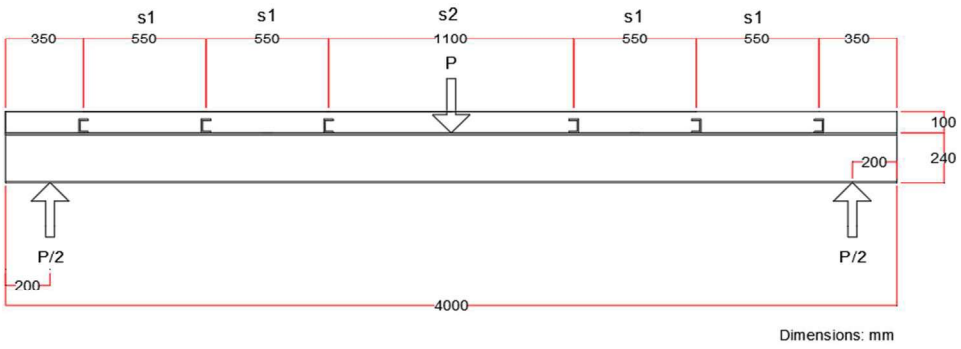

Figure 3.6. Details of test specimen 3 and 4 (side view)

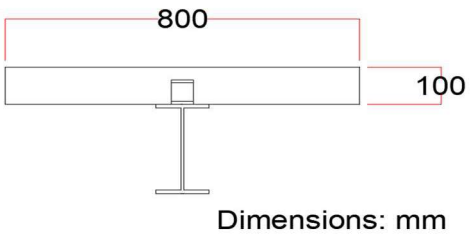

Figure 3.7. Details of test specimens (front view)

3.1.2. Tensile Strength of Steel used in Specimens

The yield strength of steel beams was determined by testing of six coupon samples taken from web and flange of steel beams used in the test specimens. The stress-strain behavior obtained from tension coupon tests and the yield strength values are given in Figure 3.8 and Table 3.2. The yield strength was calculated by taking the values at deformation point of %0.2. As seen from this table, the average of yield strength of

web and flange are 300 and 287 MPa, respectively. As these values are closer to each other, the average of all data is used. Results of these tension tests indicated the yield strength of 293.9 MPa with standard deviation of 7.61 MPa.

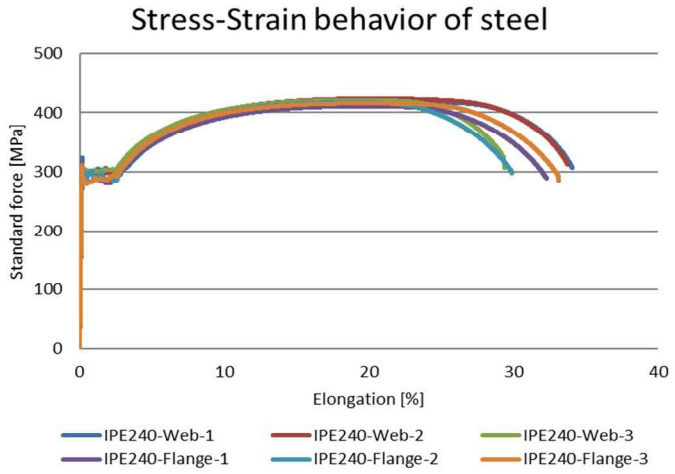

Figure 3.8. Stress-strain behavior of steel used in specimen

Table 3.2. The yield strength of coupons

Web or Flange:	E (GPa)	Fy @ %0.2 (MPa)	Fy @ %0.6 (MPa)	Fy (lower yield strength) (MPa)	Fy (upper yield strength) (MPa)	Fu (MPa)
Web-1	184.24	299.00	296.56	295.46	324.35	419.27
Web-2	194.54	300.60	299.44	294.74	313.79	423.29
Web-3	199.52	302.63	301.86	300.56	309.76	420.98
Average:	192.77	300.74	299.29	296.92	315.97	421.18
Standard Deviation:	6.36	1.49	2.16	2.59	6.15	1.65
Flange-1	196.04	283.39	283.75	279.70	291.16	410.71
Flange-2	187.26	293.33	298.94	284.06	311.95	417.40
Flange-3	190.85	284.43	281.35	279.35	311.52	415.67
Average:	191.38	287.05	288.02	281.04	304.88	414.59
Standard Deviation:	3.61	4.46	7.79	2.14	9.70	2.84
All data: Average:	192.07	293.90	293.65	288.98	310.42	417.89
Standard Deviation:	5.22	7.61	8.03	8.29	9.83	4.03

3.1.3. Mix Proportion and Compressive Strength of Filling Materials

The nominal mix proportions of filling materials were the same with the ones used in push-out tests. The compressive capacities of these materials can be found in Table 3.3.

Table 3.3. The compressive capacities of filling materials in shear pockets

Compressive Strength of Filling Materials in Shear Pockets			
High Strength Mortar (Specimen 1&4)			
Time after casting:	fc cylinder (MPa)	fc cube (50x50x50mm) (MPa)	fc cube (150x150x150mm) (MPa)
Day 28	46.05	-	54.75
Test day	47.25	53.93	58.59
Low Strength Mortar (Specimen 3)			
Time after casting:	fc cylinder (MPa)	fc cube (50x50x50mm) (MPa)	fc cube (150x150x150mm) (MPa)
Day 28	26.65	-	32.35
Test day	28.22	32.43	34.65
Grout (Specimen 2)			
Time after casting:	fc cylinder (MPa)	fc cube (50x50x50mm) (MPa)	fc cube (150x150x150mm) (MPa)
Day 28	53.66	-	63.85
Test day	53.76	66.03	66.10

3.2. Beam Test Setup

The test setup for testing of beam specimens can be seen in Figure 3.9 and Figure 3.10. The piston, loadcell and load spreader placed with the help of a hinge are shown in Figure 3.11. There is one LVDT with a maximum capacity of 150 mm and five strain gages placed at the mid-span of beam as indicated in Figure 3.12. Moreover, there are two LVDTs with a maximum capacity of 30 mm placed at both ends of composite beam specimen to measure the slip between precast deck and steel section. This LVDT detail and the hinge formation can be seen in Figure 3.13. The hinge of beam specimens was designed by using UPN80 profile and a cylindrical steel plate.

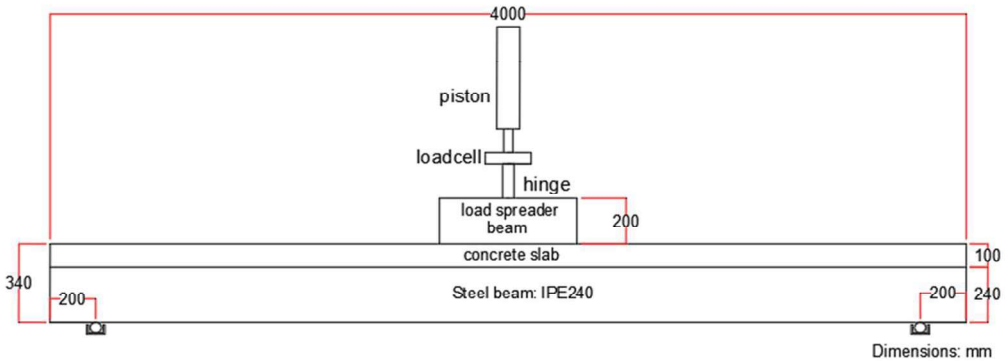

Figure 3.9. Details of beam test setup

Figure 3.10. The beam test setup

Figure 3.11. The piston, load cell and load spreader detail

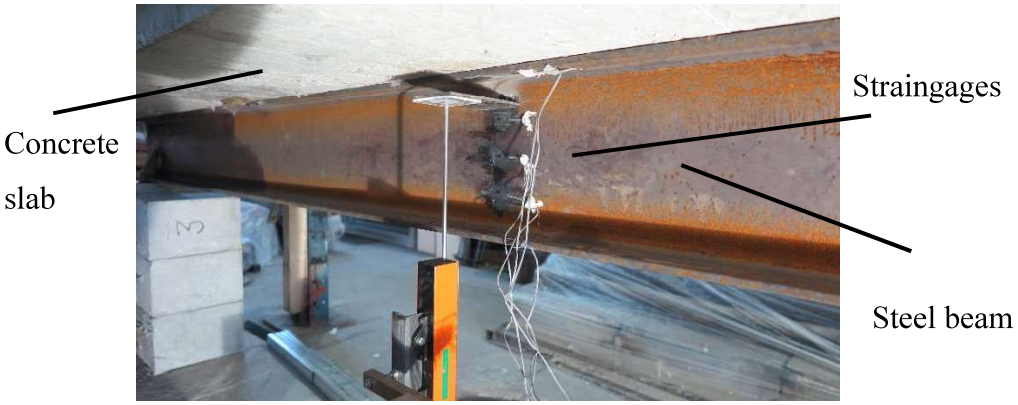

Figure 3.12. LVDT measuring mid-span deflection and strain gage detail

Figure 3.13. LVDT measuring slip between concrete and steel and hinge detail

3.3. Test Results

The test results of beam tests have been classified as failure mode and moment-deflection response, respectively.

3.3.1. Failure Mode

In general, all composite specimens showed similar flexural response which includes yielding at the mid-span of steel section, damage at the mid-span of the concrete deck, and cracking pattern concentrated around the shear pockets. The typical failure of a composite specimen and the yielding of steel section can be seen in Figure 3.14 and

Figure 3.15, respectively. The concrete cracking can also be seen in Figure 3.16. These cracking patterns and slab damage were present in all of the specimens, but separation between concrete and steel sections also occurred in the third specimen with a degree of composite action of 0.66 as seen in Figure 3.17.

Figure 3.14. Typical deformed shape of composite beam (Specimen-1)

Figure 3.15. Yielding of steel section observed during bending test (Specimen-2)

Figure 3.16. Concrete crushing below loading beam (Specimen-4)

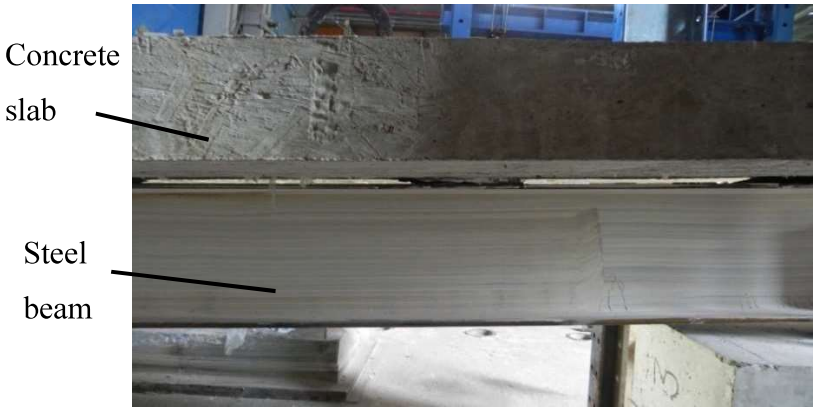

Figure 3.17. Separation between deck and steel at the end of test of Specimen-3

3.3.2. Moment-Deflection Response

The influence of the degree of partial composite action on moment capacity of specimens is summarized in Table 3.4. The calculated capacity of each specimen was obtained with the solution method of the study of Baran&Topkaya (2014).

To calculate the predicted moment capacity, the first step was to find the depth of concrete slab with the formulation in Equation 3.2. Then, the plastic neutral axis of each specimen with variable degree of composite action was found. The stress and force distribution on a typical beam can be seen in Figure 3.18. The depth of concrete slab subjected to compression for fully or partially composite action and the places of plastic neutral axis for each specimen can be found in Table 3.5. Afterwards, the compressive and tension forces at each side of plastic neutral axis were calculated for each specimen to find the total moment capacity.

$$a = \frac{\min(A_s F_y, 0.85 f_c^{'} A_c, \sum Q_n)}{0.85 f_c^{'} b} \qquad (3.2)$$

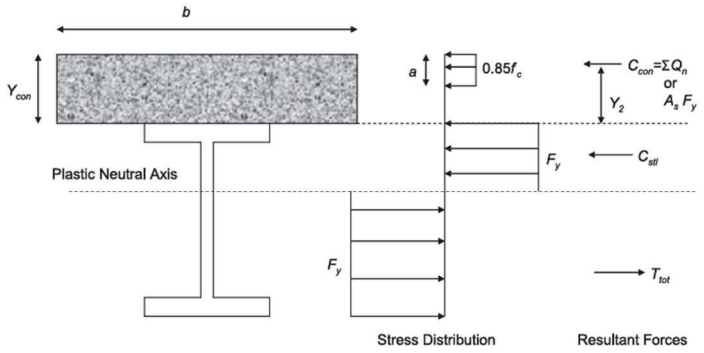

Figure 3.18. Stress and force distribution on a typical composite beam (Baran & Topkaya, 2014)

Table 3.4. Summary of experimental results

Specimen #	Specimen name	Connector Strength, Q_n (kN)	Calculated capacity, M_u (kN.m)	Measured capacity, M_u (kN.m)	Measured/ Calculated
1	UPN65-M1-50-C2	302	190.09	183.64	0.97
2	UPN65-G-50-C2	319	192.21	183.42	0.95
3	UPN65-M2-50-C3	255	201.17	171.72	0.85
4	UPN65-M1-75-C3	414	221.48	204.28	0.92

Table 3.5. The plastic neutral axes of beam specimens

Specimen	$0.85*f_c*A_c$ (kN)	F_y*A_s (N)	ΣQ_n (kN)	a (mm)	PNA (mm)	PNA:
UPN65-M1-50-C2	2221.56	1149.13	604	27.19	7.73	on steel top flange
UPN65-G-50-C2	2146.08	1149.13	638	29.73	7.25	on steel top flange
UPN65-M2-50-C3	2212.72	1149.13	765	34.57	5.45	on steel top flange
UPN65-M1-75-C3	2107.32	1149.13	1242	54.53	0	on concrete

PNA: from bottom of concrete

The results show that calculated and measured capacities are close to each other. The measured capacity of the third specimen is lower than the expected value. This is because of the separation between concrete and steel of this specimen.

3.3.2.1. Moment-Midspan Deflection Response

The moment versus midspan deflection of each beam specimen can be investigated in Figure 3.19. The moment-deflection behavior and the deflection values are similar for all specimens. The increase of the degree of composite action influenced the moment capacity as observed.

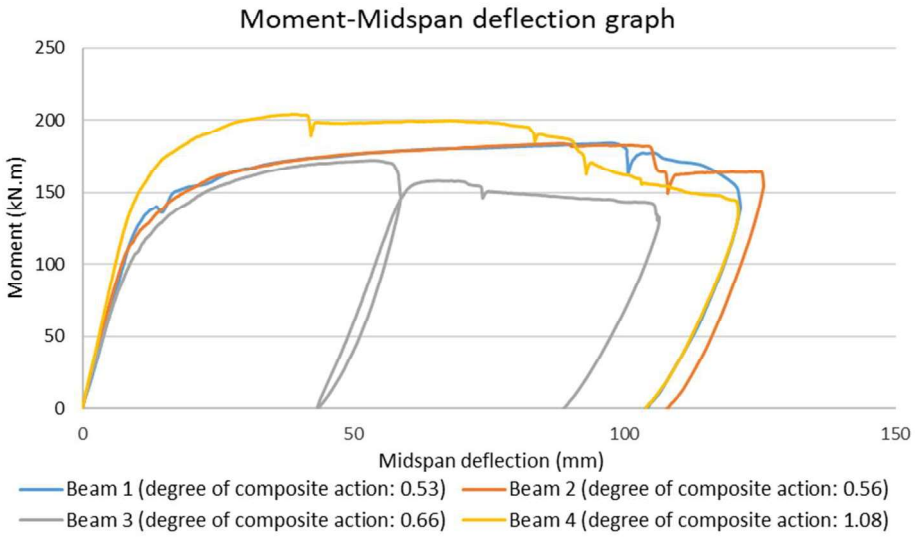

Figure 3.19. Applied moment versus mid-span deflection response of specimens

3.3.2.2. Steel-Concrete Interface Slip

The variation of the slip of concrete slab relative to the steel beam measured at two ends of specimens can be seen in Figure 3.20, Figure 3.21, Figure 3.22, and Figure 3.23 for specimen 1, 2, 3, and 4, respectively.

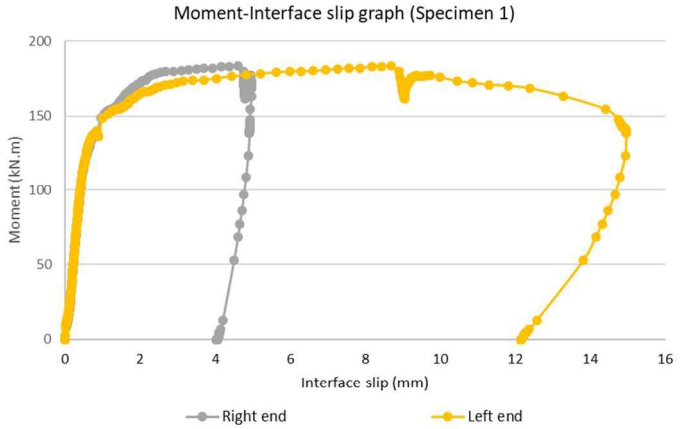

Figure 3.20. Applied moment versus interface slip response of specimen 1

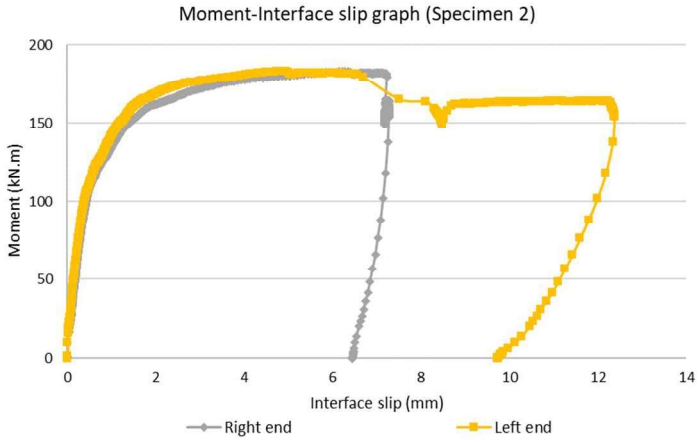

Figure 3.21. Applied moment versus interface slip response of specimen 2

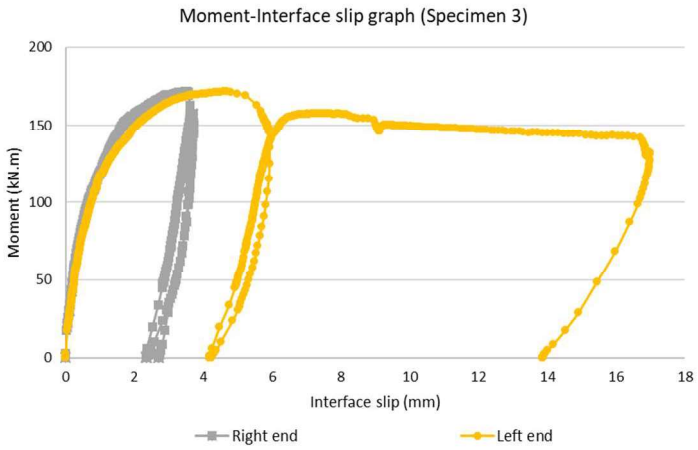

Figure 3.22. Applied moment versus interface slip response of specimen 3

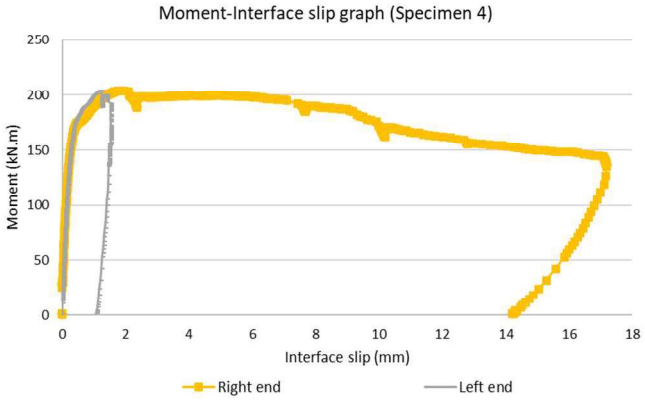

Figure 3.23. Applied moment versus interface slip response of specimen 4

The total amount of slip that occurred at each end of specimens at the end of load tests was not equal. One end of the concrete slab underwent excessive slip, while the slip at the other end remained much smaller. The excessive slip was observed at the same side that had extensive concrete slab cracking.

3.3.2.3. Strain Profile through Beam Depth

Variation of the cross section strains in the composite beam specimens are given in Figure 3.24. The plots indicate linear elastic strain profiles, where strains measured under an applied moment of only 20 kN.m were used to construct the strain profiles.

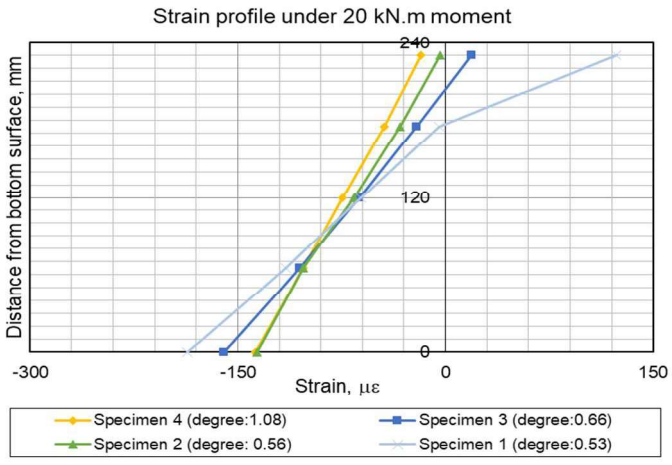

Figure 3.24. Strain profile through steel beam under 20 kN.m moment

The plots clearly indicate that the elastic neutral axis, which was indicated by zero strain on the strain profile, moves up as the degree of composite action increases. This behavior matches up with the conventional deck specimens tested in the study of Baran&Topkaya (2014). It means that the strain behavior does not change with the type of deck of composite specimen.

To sum up, the precast deck-steel composite specimen with channel shear connector works reasonably well in various degree of composite action as seen in this study.

CHAPTER 4

SUMMARY, CONCLUSION AND FUTURE RECOMMENDATIONS

The use of channel connectors in precast slabs has not been investigated in the studies about composite systems as demonstrated in the literature review. This research aimed to evaluate the behavior of precast deck-steel composite systems when the precast decks are connected to the steel beams with channel shear connectors, and the shear pockets around channel shear connectors are filled with materials like mortar or grout.

In the first phase of this study, twenty push-out tests were performed on specimens with monotonic loading including European channel shear connectors with various channel height, channel length, type and capacity of filling material. The interval of channel height was between 65 and 140 mm, and channel length was 50 and 75 mm used for each channel height, separately. The filling materials in shear pockets to reach composite action were high strength mortar, low strength mortar and grout. The push-out test setup was different than the standard one because the present test setup was in a horizontal plane and the specimens were half of the classical one with the aim of practicability, cost and time saving. No distinct difference was detected in the deformation pattern of specimens with different parameters. The failure mode was the fracture of channel shear connectors near the fillet between the web and the flange. The push-out load and slip capacity increases with channel height, width and capacity of filling material. The empirical equation of Baran&Topkaya (2012) developed for conventional connectors were found to provide conservative estimates of the connectors embedded in mortar or grout.

In the second phase of the present study, four beam tests were conducted on specimens to obtain the flexural behavior of precast deck-steel composite beams connected with channel shear connectors welded on steel sections. The degree of composite action

was changed from partial to fully composite case. Higher degree of partial composite action increased the moment capacity of composite beam specimens, without any major influence on the general response under flexural loading. However, premature separation between precast concrete and steel occurred in the third composite beam specimen which has a degree of composite action of 0.66, so its moment capacity was much lower than expected. For this reason, the axial strength of channel connectors embedded in mortar or grout should be studied in the future.

In general, the measured and calculated capacities are close to each other for partially and fully composite beams. However, the measured capacities are slightly lower than the calculated ones indicating that the calculation method is on the non-conservative side. The level of non-conservatism is even more pronounced if higher connector strengths are used in the calculations. In its present form, the connectors strength obtained from the push-out tests were used in the resistance calculations. When the strength of filling materials are examined, it can be observed that the strength of high strength mortar used in specimens 1 and 4 have 9.15% higher capacity than its counterpart in push-out tests. Similarly, the strength of grout used in specimen 2 has 20.8% higher than its counterpart in push-out test. For low strength mortar the compressive strength obtained in beam test and pus-out tests were similar. Based on this observation it can be concluded that more detailed analysis of these partially and fully composite beams are needed to investigate the sources of non-conservatism. It should be mentioned that differences increase as the degree of composite action increases. The same trend is also present in the tests conducted by Baran&Topkaya (2014) where the deck is conventional in-situ concrete. In these tests the measured to calculated capacity ratios decreased from 1.11 to 0.97 as the degree of composite action increased from 0.35 to 1.06.

As a recommendation to the future studies, precast deck-steel composite structures with bolted channel shear connectors should be developed and push-out and beam tests should be conducted to investigate the behavior of bolted connections. It provides

improvement on connection from welded to the bolted one, and the advantages of bolted connections can be obtained in this proposed system.

REFERENCES

AISC, Specification for Structural Steel Buildings, American Institute of Steel Construction, Chicago, Illinois, 2005.

Al-Darzi, S. Y. K., Chen, A. (2006). "Conceptual Design and Analysis of Steel-Concrete Composite Bridges: State of the Art" Steel Structures, 6, 393-407.

Baran, E., and Topkaya, C. (2012). "An experimental study on channel type shear connectors." Journal of Constructional Steel Research, 74, 108–117.

Baran, E., and Topkaya, C. (2014). "Behavior of steel–concrete partially composite beams with channel type shear connectors." Journal of Constructional Steel Research, 97, 69–78.

CSA, Limit States Design of Steel Structures, CSA Standard CAN/CSA S16-01, Canadian Standards Association (CSA), Toronto, Ontario, 2001.

Kim, Y.-C., Shin, S., and Park, J.-J. (2003). "Shear and fatigue strength of grout-type transverse joints." Canadian Journal of Civil Engineering, 30(4), 607–614.

Lam, D., Elliott, K., and Nethercot, D. (1999). "Steel — Concrete Composite Construction with Precast Concrete Hollow Core Floor." Advances in Steel Structures (ICASS 99), 459–466.

Lam, D., Elliott, K., and Nethercot, D. (2000). "Parametric study on composite steel beams with precast concrete hollow core floor slabs." Journal of Constructional Steel Research, 54(2), 283–304.

Lam, D., Elliott, K., and Nethercot, D. (2000). "Experiments on composite steel beams with precast concrete hollow core floor slabs" Proceedings of the Institution of Civil Engineers - Structures and Buildings, 140(2), 127-138.

Lam, D., Elliott, K., and Nethercot, D. (2000). "Designing composite steel beams with precast concrete hollow-core slabs" Proceedings of the Institution of Civil Engineers - Structures and Buildings, 140(2), 139-149.

Lam, D. (2002). "Composite steel beams with precast hollow core slabs: behaviour and design." Progress in Structural Engineering and Materials, 4(2), 179–185.

Liu, Y., Guo, L., Qu, B., and Zhang, S. (2017). "Experimental investigation on the flexural behavior of steel-concrete composite beams with U-shaped steel girders and angle connectors." Engineering Structures, 131, 492–502.

Qureshi, J., Lam, D., and Ye, J. (2011). "Effect of shear connector spacing and layout on the shear connector capacity in composite beams." Journal of Constructional Steel Research, 67(4), 706–719.

Pashan, A., and Hosain, M. U. (2009). "New design equations for channel shear connectors in composite beams." Canadian Journal of Civil Engineering, 36(9), 1435–1443.

Shariati, A. (2012). "Various types of shear connectors in composite structures: A review." International Journal of the Physical Sciences, 7(22).

Shariati, M., Sulong, N. R., Suhatril, M., Shariati, A., Khanouki, M. A., and Sinaei, H. (2013). "Comparison of behaviour between channel and angle shear connectors under monotonic and fully reversed cyclic loading." Construction and Building Materials, 38, 582–593.

Shim, C.-S., Lee, P.-G., and Chang, S.-P. (2001). "Design of shear connection in composite steel and concrete bridges with precast decks." Journal of Constructional Steel Research, 57(3), 203–219.

Şamhal, E. (2005). "Lecture 1.1: Composite construction, General." SSEDTA European Steel Computer Aided Learning, 1–34.

Topkaya, C., Yura, J. A., and Williamson, E. B. (2004). “Composite Shear Stud Strength at Early Concrete Ages.” Journal of Structural Engineering, 130(6), 952–960.

Viest, I.M., Colaco, J.P., Furlong, R.W., Griffis, L.G., Leon, R.T., and Wiley, L.A.. (1997) “Composite Construction Design for Buildings”. ASCE Publications, McGraw-Hill.

Viest, I.M., Siess, C.P., Appleton, J.H., and Newmark, N.M.. (1952). “Full-Scale Tests of Channel Shear Connectors and Composite T-Beams”. University of Illinois Bulletin No: 405,Urbana, IL.